"In presenting the dissertation as a partial fulfillment of the requirements for an advanced degree from the Georgia Institute of Technology, I agree that the Library of the Institution shall make it available for inspection and circulation in accordance with its regulations governing materials of this type. I agree that permission to copy from, or to publish from, this dissertation may be granted by the professor under whose direction it was written, or, in his absence, by the dean of the Graduate Division when such copying or publication is solely for scholarly purposes and does not involve potential financial gain. It is understood that any copying from, or publication of, this dissertation which involves potential financial gain will not be allowed without written permission.

_____

_____

6

COMPARISON OF VIDEO DETECTORS FOR THE MILLIMETER WAVELENGTHS

A THESIS

Presented to

the Faculty of the Graduate Division

by

Alfred Carlton Daniel

In Partial Fulfillment

of the Requirements for the Degree

Master of Science in Electrical Engineering

Georgia Institute of Technology

September 1957

5R
12R

COMPARISON OF VIDEO DETECTORS FOR THE MILLIMETER WAVELENGTHS

Approved:

Thesis Advisor

Date Approved by Chairman: September 16, 1952

ACKNOWLEDGMENTS

I wish to express my sincere appreciation to Dr. F. K. Hurd, thesis advisor, and to Dr. J. Q. Williams and Mr. M. E. Meadows, Jr., for their valuable criticism and guidance throughout the preparation of this thesis. Also, I wish to acknowledge the assistance provided by the Engineering Experiment Station of the Georgia Institute of Technology through the use of its laboratory facilities. Finally, I wish to extend my thanks to my wife, Lena, for her encouragement and sacrifices during my tenure of study at the Georgia Institute of Technology.

TABLE OF CONTENTS

LIST OF TABLES

LIST OF ILLUSTRATIONS

Figure | Page

ABSTRACT

In many microwave applications of direct or video detection there is a choice in the type of instrument to be used. Two of the more common devices for these applications are the silicon crystal diode and the hot wire bolometer (or the barretter). The purpose of this investigation was to study in detail the several characteristics of these two detectors, to substantiate through laboratory experiments the general behavior of the detectors as predicted by the given theory, and in general to summarize the relative characteristics of the two detectors within the frequency limits of most present-day equipment.

The dynamic square-law response, the frequency response, and the sensitivity are given as the primary characteristics of the video detector for most microwave applications. These factors and their influencing detector parameters are discussed for both detectors, and several possible methods for improvement are considered. Typical curves are given to demonstrate the dependence of the detector performance on such parameters as the video load resistance, impedance mismatch, and video bias for the crystal; and the time constant and pulse width for the barretter. The advantages and limitations of these detectors in several of the frequently used applications are discussed in detail.

CHAPTER I

INTRODUCTION

Definition of Video Detection.--Video detection may be defined as the process of recovering from a modulated wave a voltage or current that varies in accordance with the modulation present on the wave(1).* This detection process may be performed by any one of several devices. Experimental and theoretical discussion of various facets of the operation of these devices has appeared in widely scattered publications. The objective of this investigation is to formulate from the existing theory and from any necessary laboratory experimentation a comprehensive functional description and relative comparison of the two devices most often used as microwave video detectors--the crystal and the bolometer. This thesis will present in a single discussion a comparative description of these two detectors that will assist in their proper utilization, and it will also point out the means by which optimum video detection performance may be effected.

First, before discussing these detection devices, it is necessary to describe the factors that will best characterize the video detector.

---

*Numbers in parentheses refer to the bibliography.

Modulation detection implies a means of detecting and transferring to the output terminals the envelope of a given signal, thus possibly requiring a system of large video bandwidth for good signal fidelity. However, this is not always the case. Depending upon the particular application, the required bandwidth may vary from a few cycles to a bandwidth in the order of megacycles. Thus, the video bandwidth required of the system is an important characteristic in defining the detector performance and has a large influence upon the selection of the detection device. Another factor directly related to the video bandwidth, but often discussed separately, is the video response of the detection system. This response is a measure of the ability of the system to reproduce the envelope of the modulation contained within the applied signal. For pulse modulation this response may be defined in terms of rise time; otherwise it is necessary to consider the frequency spectrum of the detected signal. The video response of the system output may vary over wide limits. For applications such as envelope detection it is desirable to have true modulation reproduction, while in certain laboratory measurements it is only necessary to establish a correspondence between the applied signal and the detector output.

The direct detection employed by the video-detection system differs from the mixer or superheterodyne system in that there is no local oscillator to apply a constant signal

power to the detector for maintaining an a-c bias about a particular power level and to provide a means of generating an intermediate frequency. Thus, the direct detector is a simpler system that does not have the additional complexity introduced by the local oscillator and intermediate-frequency (i-f) and possibly radio-frequency (r-f) amplifiers. But to compensate for this simplicity, the performance of the direct detector with no local biasing oscillator is dependent upon the amplitude of the applied signal. While the mixer crystal detector always functions in its linear detection range, the video detector is not restricted in this manner; the possible useful dynamic range of the video detector is determined by its known dynamic response, usually in the low-level square-law region. Hence, a third important video detector characteristic is the dynamic detection law.

A last important characteristic is the sensitivity of the detector. This sensitivity describes the ability of the detection device to produce an output for a given input variation. Although the sensitivity of the several video detectors will vary considerably, the direct detection system has a poor sensitivity as compared with that of the superheterodyne system; this difference may be as great as 40 db(2). Also associated with the detector sensitivity is the minimum detectable signal, a characteristic determined by the sensitivity and the noise level of the system. A means often used to describe this minimum power level is the tangential signal

sensitivity, defined as the amount of signal power below a one milliwatt reference required to produce an output pulse whose amplitude is sufficient to raise the noise fluctuation by an amount equal to the average noise level.

To summarize, four important characteristics of the direct detection system are:

1. bandwidth
2. video response
3. dynamic detection law
4. sensitivity

These factors are interrelated and it is not always possible to obtain the optimum of two or more of them simultaneously.

Detection Elements.--At present several devices are employed as video detectors. The diode rectifier is ordinarily used for most applications of direct video detection of amplitude modulated waves. At the lower frequencies where the transit-time effects are negligible, the diode vacuum tube is the most popular detection device. At the higher frequencies and into the millimeter wavelength region the silicon crystal diode, a point-contact type semiconductor rectifier, is the most frequently employed. The next most common group of devices used for video detection is considered under the general classification of bolometers, or thermally sensitive detectors. This group is further subdivided according to the polarity of the temperature coefficient of resistivity: the thermistor with a negative coefficient and the barretter with a positive

coefficient. The barretter includes such elements as the Wollaston wire bolometer, selected fuses and metallic films. While the crystal demodulation process depends upon the crystal rectification characteristics, the bolometer demodulation results from its change in resistance as it absorbs power. A study of these two methods of video detection and their performance characteristics is the purpose of this study. Instead of considering the group of bolometers as a whole, only the Wollaston wire bolometer will be discussed and will henceforth be more simply referred to as the barretter. The Wollaston wire bolometer has certain advantages over the other thermal detectors and is thus more frequently used at the microwave frequencies.

In addition to the microwave video detectors named above, there are several other detectors that are used to varying degrees. The thermistor may be used in the same manner as the barretter except that it is limited by a much larger thermal time constant. Several other devices normally considered only as infrared and heat detectors have been used successfully at the millimeter wavelengths; these include such instruments as the thermocouple, the termopile and the Golay cell(3). Also, recently a crystal detector constructed in the form of a wafer to be mounted across the waveguide has been developed by Bell Telephone Laboratories(4). This detector and mount is intended to eliminate the need for tuning adjustments and to make the crystal and mount less frequency

sensitive. Although the unit was designed primarily as a mixer detector for the four to seven millimeter wavelength region, it has been used successfully as a video detector to wavelengths as short as 2.8 millimeters. This crystal detector was not available during this investigation.

The Objective.--The largest void in the frequency spectrum at the present exists between the rather familiar wavelengths normally associated with radar and those of infrared. The objective of this study is to summarize in one paper the known operational characteristics of the silicon crystal and the Wollaston wire bolometer (or barretter) as applied to the problems of video detection and to extend the generalization of these characteristics by justification through laboratory experiments to the highest available frequencies that are now being considered for radar and similar applications. The relative utility of these two detectors will be based upon the several characteristics of each as applied to specific types of video detection applications rather than by direct laboratory comparisons; this procedure will be seen to be justified because the dissimilarity between the two detectors gives each an area of superiority. The maximum dynamic limit for the detector characteristics to be discussed here will be approximately 10 milliwatts (-10 dbm)* and the frequency range will

*The dbm is a measure of the power level in decibels with 1 milliwatt equivalent to 0 dbm as the reference power level.

be from 10,000 mc. (3 cm. wavelength) to 70,000 mc. (0.43 cm. wavelength).

CHAPTER II

THE CRYSTAL-VIDEO DETECTOR

General Characteristics.--The crystal diode is the most often used device for video detection at the microwave frequencies. This degree of acceptance is due to the relatively good sensitivity and small size that characterize the crystal as a video detector.

Since this discussion is limited to only the video detector, it is desirable to compare some of the general characteristics of the crystal-video system with those of the crystal-mixer system. Several rather prominent differences will be noted. The crystals designed specifically for the low power-level operation, normally required for the video detector, are very similar to those used as mixer detectors. However, the crystal-video detector has a more sensitive contact point on the crystal and is therefore more susceptible to burnout and mechanical breakage than the mixer crystal. This additional fragility must be tolerated to increase the signal sensitivity of the video detector; this increased sensitivity is required because of the overall lower sensitivity of the video-crystal system as compared with the mixer-crystal system. The mixer-crystal system is able to obtain a considerably better signal-to-noise ratio through its associated i-f amplifiers than is possible with the video detector and its amplifier.

The video system does have the advantage of a much wider r-f bandwidth; the limits are determined for the most part by the detector itself. Because of the high gain normally required of the video amplifier, the video system does not have as good a video response as possible with the mixer system. In addition, if good frequency selectivity is required of the video system, additional filtering is desirable at the input to the detector. Thus, use of the crystal-video system is limited to applications that do not require either very high sensitivity or very good pulse reproduction.

The ideal low-level crystal-video detector is a square-law device. Because of this square-law characteristic the video amplifier must have twice the dynamic range of the video detector, that is, for the video system to have a dynamic response of 60 db, the video amplifier must have a dynamic response of 120 db. With the square-law detection, two voltage signals compared at the video output will differ by twice the voltage difference at the microwave input to the detector. This effect results in a two-fold greater signal-to-noise ratio for the square-law device compared with the linear detector for any given gain and noise characteristics. Hence, a change in the system bandwidth will affect the minimum noise level of the video system; however, this effect will be only half as great as with the linear detector.

The microwave crystal detector is a semiconductor, usually silicon, with a tungsten catwhisker all encased in one

of several standard mounts(5). The two most common types of mount construction are the cartridge and the coaxial mounts. The coaxial mount is generally employed at frequencies of 10,000 mc. and higher because of the minimization of mechanical effects.

Figure of Merit.--One method that has come into popular usage for characterizing the performance of the crystal-video detector is the figure of merit, M. The noise figure, a sensitivity factor associated with crystal-mixer applications has no meaning for the square-law detector, whose noise is a function of the signal level and bandwidth. Instead, a figure of merit that is proportional to the signal-to-noise ratio of the crystal has been defined(5) as

$$M = \frac{BR_V}{\sqrt{R_V + R_a}}$$

where B = current sensitivity of the crystal

R_V = crystal video resistance

R_a = amplifier equivalent noise resistance.

However, this method of describing the crystal-video system has certain disadvantages for many applications, particularly for low level signal detection and envelope viewing. The figure of merit yields information on the system performance only at a particular power level, and thus does not give a complete description of the crystal operation. For completeness a short derivation of the figure of merit is included in Appendix 1.

Detection Law.--Although this discussion is limited to a comparison of two approximately square-law detectors, it is desirable to consider the relationship that exists between the idealized linear and square-law detectors. The detected video power of the perfect linear detector is directly proportional to the applied microwave modulated power permitting complete energy conversion under ideal conditions. However, this direct proportionality does not exist with the square-law detectors; the detected video power is related to the square of the applied microwave power. This squared relationship would allow the square-law detector to become a power source if it were valid for values of the applied microwave power above a certain maximum limit. Thus, in contrast to the linear detector, the ideal square-law detector has a maximum microwave power limit at which it may be operated. In general, this upper limit for the ideal square-law range is not fixed but is dependent upon the other detector characteristics. This maximum power limit corresponds to the point at which there is complete power transfer by the detector, or ideal linear detection. Hence, the square-law detector must always function in a power region where the efficiency of the detection process is variable and less than 100 per cent, even for the ideal case.

Fig. 1 shows an idealized graph for square-law and linear detection. The region above curve A corresponds to power generation while that below curve A corresponds to power loss. Hence, the maximum range of the square-law detector is

shown to be the limiting value on curve A where the square-law detector functions as a linear device. From Fig. 1 a square-law relationship may be obtained as

$$\log P_V = 2 (\log P_M - \log P_R)$$

where P_V = detected video power

P_M = applied microwave power

P_R = arbitrarily chosen reference point on Fig. 1.

This equation reduces to

$$P_V = \left(\frac{P_M}{P_R}\right)^2 = KP_M^2 \qquad (1)$$

where $K = \frac{1}{R_R^2}$ is a factor that determines the region of square-law operation and is dependent upon the detector characteristics.

The performance of the square-law detector may be partially described by the parameter K or P_R. Depending upon the value of K, it is possible to shift the square-law detection curve along the P_M axis giving possible characteristic curves such as B and C in Fig. 1. It is possible, therefore, to control the maximum limit of the permissible applied power for square-law response, that is the dynamic range, by varying K. In addition, if the P_M axis of Fig. 1 is considered as the lower practical limit set by the video noise of the detection system, it is obvious that the minimum detectable signal is also dependent upon K. Then, in general, it is not possible to obtain simultaneously both a wide dynamic response and a low limit to the minimum detectable power with a given detector.

If the applied power, P_M, were to increase beyond the value given for the limit of the ideal square-law range, the perfect square-law detector would "break" from its square-law mode of operation and continue as a linear detector. The detector would go from a square-law power region of varying efficiency to one in the ideal case of 100 per cent efficiency. In practice this result is approximated by the crystal, that is as the applied power is increased there is a transition from the square-law to the linear mode of operation. This transition, however, is not as simple as indicated in the ideal case. Some devices may be operated as a square-law detector but not as a linear detector; the bolometer is an example. If it is not possible for the detector to function with a linear detection law, it is necessary that another physical limit be reached before the square-law response of the detector reaches its maximum power limit at the point of linear detection. For the bolometer, this would correspond to burnout.

The above discussion is not practical in that the effect of losses is neglected. These losses will not permit the simple relationship between the square-law and the linear modes of operation as described above. The true crystal detection law response may be divided into a region of low power level square-law response, a transitional region, and a region of linear response without the direct proportionality of the ideal case. It has been shown by the simple semiconductor

theory (5) that in the square-law region and into part of the transitional region (up to approximately -30 dbm) the voltage-current characteristics of the crystal may be related by

$$i_o = A(e^{BV} - 1) \qquad (2)$$

where i_o = current generated by the crystal
V = voltage applied across the crystal
A and B = factors independent of the applied power that describe the crystal and its impedance relation to the remaining circuit.

A Taylor series expansion for equation (1) about some given operating point gives

$$i_o = A\left(BV - \frac{B^2V^2}{2!} - \frac{B^3V^3}{3!} - - - - \right)$$

The square-law characteristics may best be demonstrated by assuming an applied sinusoidal voltage, $V = V_o \sin wt$. This voltage substituted into the above equation gives

$$i_o = A\left[BV_o \sin wt - \frac{B^2V_o^2}{2\cdot 2!}(1 - \cos 2wt) - \frac{B^3V_o^3}{4\cdot 3!}\sin^3 wt - - -\right]$$

Then the d-c component is given by

$$I_o = \frac{AB^2V_o^2}{4}\left(1 + \frac{B^2V_o^2}{16} + - - - -\right) \qquad (3)$$

where I_o is the rectified output current. Note that only the even harmonics of the applied voltage are contained in the above series expansion and only these components contribute to the

demodulation current. As is to be expected with a power series expansion, as V_o increases a larger number of terms is required in the expansion to obtain a good approximation to the true result. This indicates that as V_o increases, the detector characteristics vary further from the desired square law response. For the lower power levels, as V_o approaches zero, the true square-law current response is given by

$$I_o = \frac{AB^2V_o^2}{4} \tag{4}$$

By squaring both sides of equation (4) and noting the resulting power relationship, it may be shown that this result is in the same form as equation (1). As true with equation (1), this approximate result is adequate only for the perfect square-law range and is thus restricted to the very low power levels. Equation (4) is valid only when the higher harmonic components of equation (3) may be neglected. These higher ordered components are dependent upon the applied voltage and the impedance factor B, which is related to the mismatch between the crystal and the remaining system. Therefore, the crystal response is dependent upon the parameter B as the applied power is increased beyond the upper practical square-law limit. The power-law relation for the voltage applied across the crystal and the generated current at any given power level is defined as

$$I = K_1V^L \tag{5}$$

where K_1 = constant similar to K in equation (1) that is dependent upon the detector characteristics.

L = detection law of the crystal at any given power level.

With the aid of the loglog graph of Fig. 1 it is possible to define L as

$$L = \frac{d(\log P_V)}{d(\log P_M)} \tag{6}$$

where P_V and P_M are defined with equation (1). In the transitional region between L = 2 and L = L, the detection law, L, is dependent upon B in such a manner that L may vary over rather wide limits, from the limiting value of 1 to as high as 3 or more in some instances. This range of the detection law and the deviation from the ideal response may be seen in Fig. 2. Curves B and C give the approximate practical extremes in the crystal detection law as the parameter B is varied.

The square-law detection range may be extended by making a proper choice of B in equation (3). The value of B must be chosen so that just a sufficient number of higher order terms will be present to cause curve C to extend further along the ideal square-law curve in Fig. 2. This is discussed in more detail in the next section.

It has been shown that the crystal detection law is a function of the input signal level and the constants that

describe the crystal. The result is that, except for the low power levels, the output from the crystal-video detector varies considerably from the desired square-law response, and it is not easily possible to define the power response.

Impedance Match.--The crystal detector may be considered as a two-terminal-pair network as shown in Fig. 3 where Z_m and Z_v are the microwave and video impedances as seen by the crystal, and z_m and z_v are the input and output impedances of the crystal. Usually, the crystal mount will be placed in the microwave circuit so that for any given power level it is possible to match z_m with Z_m. However, most equipment provide no means for matching z_v to the video load impedance Z_v. This problem of impedance matching is very difficult since both z_m and z_v are functions of incident microwave power level.

Since the microwave impedance, z_m, is a function of the incident power level, it is not possible to match the crystal mount to the transmission line at one value of incident power and expect this to be adequate with any fluctuation of the incident power. The microwave reflections resulting from this mismatch will result in a change in the crystal sensitivity and detection law. For proper performance of the detector, it is necessary that the input impedance to the crystal mount be readjusted at each power level to an optimum match with the transmission line. In addition, if the signal incident upon the crystal does not have rapidly changing leading and trailing edges, the effect of the varying power level at these

edges will result in a slight additional distortion of the video wave shape because of the varying input impedance match. With a reduction in sensitivity, it is possible to reduce the effect of the microwave impedance mismatch by placing a fixed resistance equal to the characteristic impedance of the transmission line in parallel with the crystal. This will reduce considerably the effect of the microwave reflections but will result in a rather large reduction in sensitivity. An approximate experimental curve showing the effect of the microwave impedance mismatch is given in Fig. 11.

The video resistance of the crystal has been found to vary approximately as shown in Fig. 4 where the maximum resistance and the slope of the curve will vary between types of crystals(6). The variations of the video-crystal detection law may be partially explained by the variations in R_v as indicated in Fig. 4. This results in a varying mismatch between the crystal and its video load. Since in equation (3) the variation in the detection law has been seen to be dependent upon the higher order terms and the factor B, the video resistance as a factor included in B will influence the detection law. Therefore, the video-crystal response is dependent to some degree upon the mismatch between the crystal and its video load. A general result has been developed (7) that relates the video load to the crystal characteristics, which may be used with reasonable accuracy in predicting the crystal performance for any given load. If the voltage applied to the

crystal is assumed to be sinusoidal, and if it is assumed that the voltage applied across the crystal is the total voltage minus the drop across the load, it is then possible through equation (2) to obtain an expression for the average detected current, I_o, in terms of the load resistance. This has been shown to result in

$$H_o\ (BV_o) = \left(\frac{BRI_o}{ABR} + 1\right) e^{BRI_o} \qquad (7)$$

where H_o is the modified Bessel function of the first kind of order zero. This result plotted for various values of load resistance compares very favorably with the true response, such as that indicated in Fig. 2 and as given in Fig. 13.

As indicated in Fig. 2, the fact that the video resistance varies with the applied microwave power may be of value in extending the dynamic square-law response of the crystal. If at the higher power levels (0 dbm) the crystal video resistance is greater than its load resistance and at the lower power levels (-30 dbm) the crystal video resistance is properly matched to its load, the curve B of Fig. 2 will follow more closely the desired square-law response. This requires a unique load impedance such that the video mismatch will result in the correct effect from the higher order terms in equation (3) to give a characteristic curve that more closely follows the square-law response. Equation (7) may be used to obtain the desired load resistance if the dynamic range of the applied signal is known. It has been found that the square-law

response may be extended 10 to 15 db by the proper choice of the load resistance(6,7). Usually in practice no attempt is made to extend the operating range of the crystal by utilizing this video mismatch. This may be partly explained by the careful choice of the load resistance that must be made and by the still relatively poor square-law detector that results after this increase in the dynamic range. Also, as may be seen by Fig. 13, there is a slight decrease in sensitivity of the video-crystal detector with the addition of the larger video load.

Frequency Sensitivity.--The video crystal is somewhat frequency sensitive; this is chiefly because of the frequency characteristics of the detector mount and the barrier capacitance of the crystal. Thus, unless the crystal is to be used at a fixed frequency it is necessary that the mount or the associated microwave circuitry be tunable. Normally the crystal mount is provided with only an adjustable waveguide plunger that will compensate for the reactive component of the microwave mismatch. The wafer type crystal mentioned in Chapter I has been designed for the purpose of decreasing the frequency sensitivity of the mount. It was found that a mismatch loss of 1.6 to 4.0 db resulted from 17 per cent change in frequency with no tuning(3).

The inherent characteristics of the crystal limit the maximum frequency that may be detected without excessive attenuation. Although the crystal barrier capacitance is considerably

less than the capacitance of other devices and is usually neglected at the lower frequencies, its effect becomes more pronounced at the higher frequencies. Commercial crystals are available with discontinuous coverage and reduced performance down to eight mm(2,3). The open waveguide type crystal detector has been used to shorter wavelengths and with greater sensitivity; but these detectors are extremely fragile and difficult to handle.

Video Response.--The video response of the crystal detector is relatively very good and it is adequate for most applications. With no load conditions the video time constant is in the order of 0.002 microseconds (8) which is more than satisfactory for most applications. However, the video response of the crystal detector is dependent upon the video output circuit in addition tothe crystal parameters. This relationship has the effect of greatly influencing the signal fidelity of the crystal detector output. In general the response of the detector is dependent upon the internal driving resistance of the crystal, the system shunt capacity, and the video load resistance. It was stated above that the optimum square-law response of the crystal is dependent upon the internal video resistance of the crystal and its load. Hence, with these opposing interacting effects it is not possible to obtain both optimum square-law response and good signal reproduction simultaneously. The best signal fidelity occurs with a very high load impedance while a load resistance

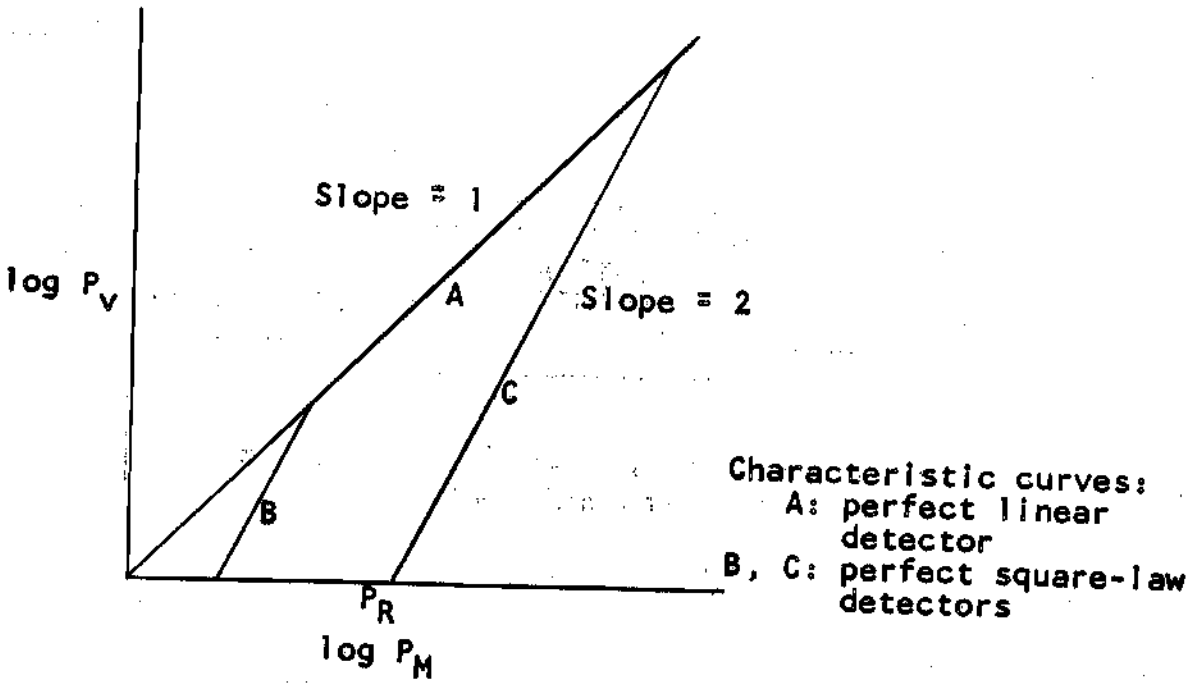

Figure 1. Idealized Comparison of Linear and Video Detection

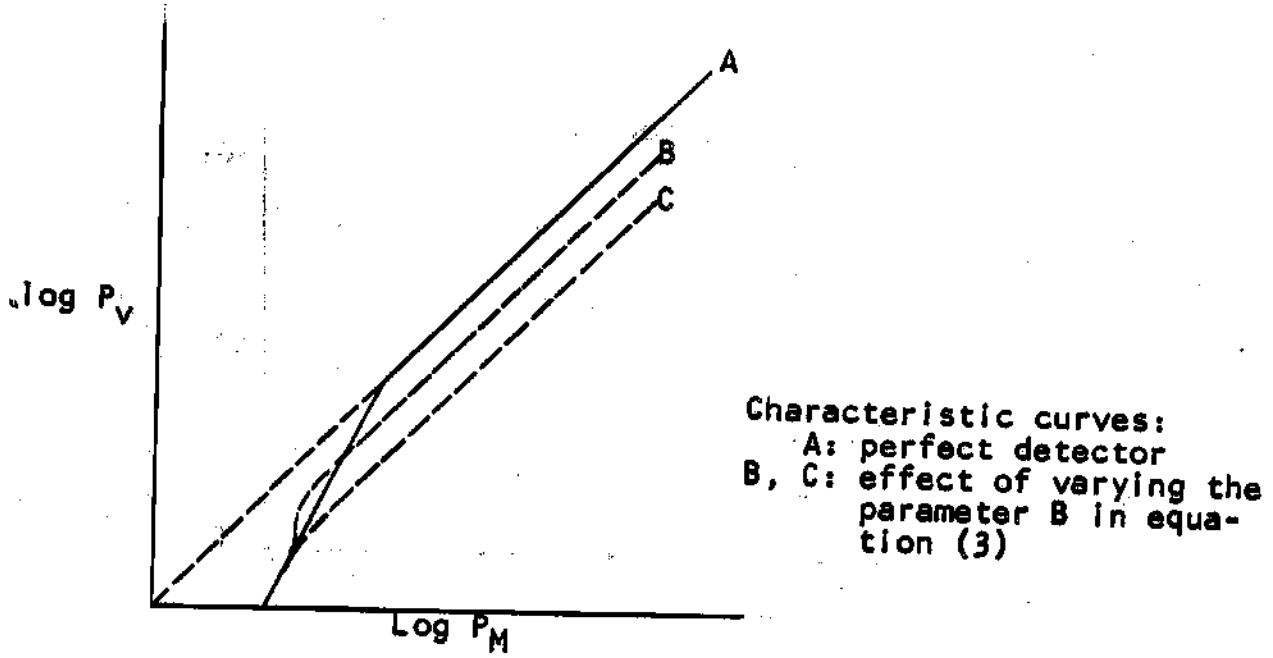

Figure 2. Crystal Detection Law

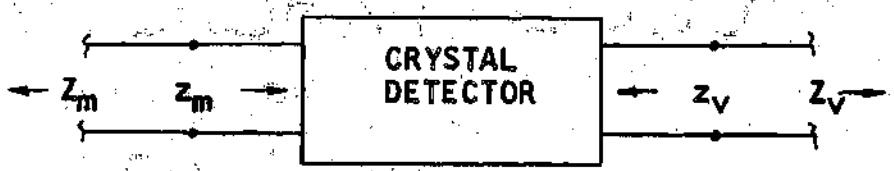

Figure 3. The Crystal Detector as a Two-Terminal-Pair Network

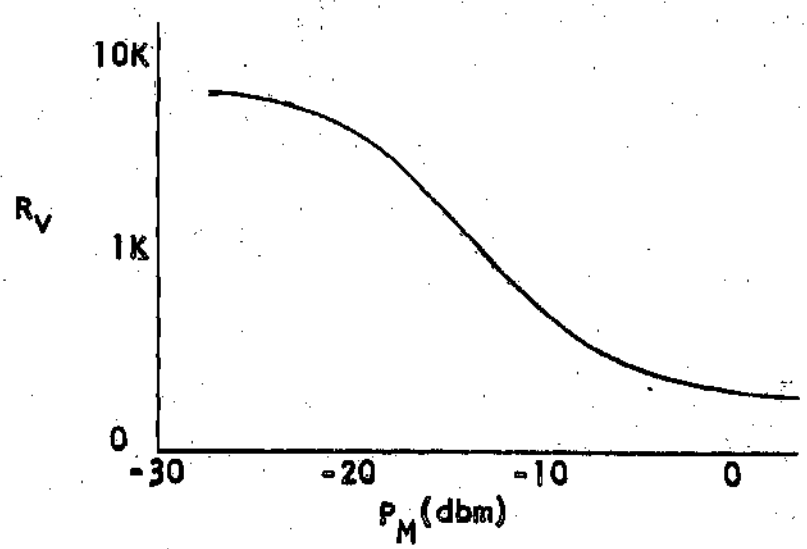

Figure 4. Typical Crystal Video Resistance Variation

of at most a few thousand ohms is required for the maximum square-law response. The effect of decreasing the load resistance is to increase the oscillatory characteristics of the crystal and its load; this result is a rapidly decaying high frequency transient superimposed on the detected output. Thus, in most practical applications a distorted output signal is to be expected from pulse envelope detection unless a very high load impedance and a resulting shorter square-law range may be tolerated.

Some improvement in the signal reproduction may be realized by applying a small positive d-c bias across the crystal. This has the effect of lowering the internal resistance of the crystal without appreciably reducing the sensitivity. A marked increase in the signal fidelity results; this may be seen in Fig. 14. Thus, it is possible to partly compensate for the increased response time of the crystal when operating with a small resistance load by the application of a small positive d-c bias.

Minimum Detectable Signal.--The minimum detected signal is a characteristic that makes the crystal more acceptable than most other devices for direct application. In addition, at the very low power levels where the crystal has the superior sensitivity, the crystal is in its operating range of approximate square-law performance.

The minimum detectable signal is normally defined as the input signal reduced to the noise level of the system,

that is the signal-to-noise ratio, S/N, is unity. In Appendix I the signal-to-noise ratio for the video crystal detector and its video amplifier is given by

$$\frac{S}{N} = \frac{MP_M}{\sqrt{4KTB_W}}$$

where M = figure of merit for the crystal at that particular power level as defined by equation (25) in Appendix I

K = Boltzman's constant

T = absolute temperature

B_W = system bandwidth

Therefore, with the incident signal power equal to the noise power the minimum detectable power level is given by

$$(P_M)min = \frac{\sqrt{4KTB_W}}{M} \qquad (8)$$

Hence, the minimum detectable signal is related to the figure of merit (or more exactly, the internal crystal video resistance to the video amplifier), the bandwidth of the system, and the frequency spectrum of the incident signal.

The crystal application and the spectrum of the incident signal will generally determine the bandwidth to be required of the system, and this will in turn establish the minimum detectable signal. For narrow-band applications such as VSWR measurements, the system bandwidth need be only sufficiently wide to pass the fundamental frequency of the incident

signal; then a correspondence may be established between the incident signal and the magnitude of the detected fundamental component. Therefore, this very narrow bandwidth allows the crystal to be used for much lower level measurements (down to the order of micromicrowatts). However, for applications involving envelope detection the bandwidth must be considerably wider and the minimum detectable signal that may be detected is thereby increased. Cheng (9) has given a relation between the pulse rise time of single and recurrent pulses and the bandwidth required to pass that pulsed signal. The rise time, t_r, of a single transient pulse is related to the system bandwidth, B_w, by

$$t_r = \frac{1}{2B_w}$$

This indicates that, as the sharpness of the pulse and the number of harmonic components is increased, the bandwidth of the system must also be increased proportionately.

Summary.--The characteristics that describe the crystal performance as a video detector may be summarized as follows:

1. The dynamic response is approximately square-law at the low power levels (noise to about -30 dbm).

2. The crystal may be used as a power-law detector over a larger dynamic range by using a calibration curve; for dependable results each crystal must be calibrated.

3. The square-law response may be extended by the

proper choice of the resistive load.

4. The crystal has a very low minimum detectable signal, as compared with other video detectors, in the order of 9×10^{-6} microwatts for a 25 cycle bandwidth.

5. Through equation (7) it is possible to theoretically determine the actual voltage applied to the crystal by the measurement of the crystal current.

6. Square-law detection and fast video response are considerably improved by using the optimum load impedance rather than the more standard 200 ohm load.

7. The detected signal fidelity may be improved with little reduction in sensitivity by applying a small positive d-c. bias.

8. It does not seem possible to obtain simultaneously both high sensitivity and square-law response over both a broad frequency and power spectrum.

CHAPTER III

THE BARRETTER VIDEO DETECTOR

General Characteristics.--The barretter to be discussed here is a very fine wire thermal detector that is normally considered under the more general heading of bolometers and is defined as a hot wire element with a positive temperature coefficient of resistivity. Usually, the barretter at the millimeter wavelengths consists of a small length of Wollaston wire with a very low thermal time constant. The Wollaston wire is constructed of a very fine thread of silver-coated platinum carefully etched so that the remaining platinum filament gives the desired ohmic resistance. The barretter construction is generally one of three types: cartridge, coaxial, and wafer. The external appearance and size of the cartridge and coaxial housing (5,8) for the barretter is similar to that for the crystal detector; this allows the interchange of the two detector elements within the same mount. At the higher frequencies the wafer type construction is more common; the mount consists of a straight section of rectangular waveguide in which the barretter is mounted across the guide between two low dielectric plates.

As desired with the crystal-video detector, the ideal microwave barretter detector has a square-law response. The barretter nearly satisfies this requirement in that it has

an approximately linear characteristic of d-c resistance versus incident power over a large portion of its resistance range. The basis of operation for the barretter is the conversion of the incident microwave power to heat within the detector element; this heat then raises the temperature of the element and causes a related change in the detector resistance. This resistance variation is observed by passing a bias current through the detector and noting either the current changes through the element or the voltage variations at the terminals of the elements.

When the barretter characteristics are described by the factors given in Chapter I, it will be observed that in many respects the crystal and barretter have opposite desirable characteristics. The wide acceptance of the barretter for some applications is because of its very good dynamic square-law response. For low and medium power levels this characteristic makes the barretter very acceptable for such uses as VSWR and impedance measurements. Again in constrast with the crystal detector, the barretter time constant is too long for the envelope detection of modulation frequencies above a few thousand cycles. Another important characteristic of the barretter is that no upper frequency limit of carrier detection exists below the infrared spectrum.

Detection Law.--The dynamic detection law of the barretter nearly approaches the ideal square-law requirement if the detector is operated with only small changes of element

temperature. This approximation is considerably better than can be obtained with the crystal or the thermistor, another thermally sensitive device in common use. The variation from the ideal square-law for the barretter is the result of certain conduction and radiation losses at the ends and along the length of the fine wire(10). In order to remove the effect of cross sectional area of the wire from the barretter parameters and to make the detector essentially independent of frequency, it is necessary that the diameter of the wire be small compared to the wavelength of the incident signal. This result is usually attainable. Thus, the power absorbed by the wire is then a function of the wire length, bias current, and construction. Although it may be shown that the barretter is not a perfect square-law detector (11), it has also been demonstrated (10) that the errors resulting from the conduction and radiation effects are almost negligible. A very thin wire mounted in air is predominantly cooled by convection, and except for the end effects, this convective cooling along the wire is substantially constant. For example, it has been shown by the above reference that the radiation loss is less than one per cent of the convection loss up to the melting point of the wire. This heat loss results in an extremely uniform radial temperature distribution and the resistance of the element is a function only of the lengthwise distribution of temperature.

Impedance Match.--The barretter and its mount must have the proper impedance match with respect to both the transmission line and the video load if proper performance is to be expected of the detector. However, this problem with the barretter is not nearly so severe as with the crystal. Where the video resistance of the crystal would change from 5000 to 1000 ohms over its operating range, the barretter will only change 10 to 20 ohms or about 5 per cent of its biased resistance. Therefore, the impedance mismatch between both the transmission line and the load does not have too great an effect upon the barretter performance. Whereas the crystal mount was by necessity tunable, the barretter is almost always operated in an untunable mount. This has the very desirable characteristic that there is no requirement for the adjustable matching elements which may introduce an additional variable error. Thus, it is necessary for the detector mount to act as a matched termination for both the transmission line and the video load. It is rather easy to construct the detector mount so that it functions as a conventional low-pass filter and presents a good match to the characteristic impedance of the line(12).

Frequency Sensitivity.--As stated above, the barretter may be so constructed that it is essentially insensitive to frequency up to its maximum design frequency; that is, the diameter of the detector element is sufficiently small so that the heating effect at the given frequency will very closely approximate the heating effect of a d-c current. Therefore, if the

barretter mount is designed with a wide v-f bandwidth, it is possible to use the barretter within the frequency limits of the mount with no additional tuning adjustments.

Video Response.--It has been shown (10,11) that the temperature variations for the barretter element may be approximated by equation (9) below with the assumptions that the barretter heat capacity, C_p, and the coefficient of heat loss to the surroundings, γ , are independent of the temperature, that the element has a uniform temperature distribution along its length, and that the heat loss to the surroundings is proportional to the temperature rise.

$$C_p \frac{d}{dt} U(t) + \gamma U(t) = P(t)$$

where u(t) and p(t) are defined respectively as the element temperature as a function of time and the microwave power applied to the barretter.

If the barretter temperature coefficient of resistivity, α , is assumed to be constant, the resistance of the barretter may be related to its temperature by

$$R_b(t) = R_o \left[1 + \alpha U(t)\right] \qquad (10)$$

where R_o is the biased resistance of the detector. The solution of equation (26) for pulsed power conditions as shown in Fig. 5a is given by equations (40) and (41) in Appendix 2; the barretter resistance as a function of time during and between

the pulses is found to be

$$R_{b1}(t) = R_o + QP_o \left(1 - e^{-\frac{t}{\tau}} \frac{1 - e^{-\frac{T-t_1}{\tau}}}{1 - e^{-\frac{T}{\tau}}} \right) \qquad (11)$$

$$\text{for } o \leq t \leq t_1$$

$$R_{b2}(t) = R_o + QP_o \left(\frac{1 - e^{-\frac{t_1}{\tau}}}{1 - e^{-\frac{T}{\tau}}} \right) e^{-\frac{t-t_1}{\tau}} \qquad (12)$$

$$\text{for } t_1 \leq t \leq T$$

where $Q = \frac{R\alpha}{\delta}$, the power sensitivity constant

τ = detector thermal time constant

t_1 = applied signal pulse width

T = period of the applied signal

From equations (11) and (12) it is possible to derive two simplified approximate solutions that will aid in the analysis of the barretter as a useful instrument for practical applications. The first solution is valid for the conditions that $t_1 \gg \tau$ and $T \geq 2t_1$, that is, assuming that the thermal time constant of the barretter is very short as compared with the pulse width of the applied power pulse and that the interval between the pulse is at least as long as the pulse itself. This requires the barretter resistance to reach its maximum value within a small fraction of the time of the applied pulse. Hence, equation (11), giving the barretter resistance during

the interval of the pulse, simplifies to

$$R_{b1}(t) = R_o + QP_o\left(1 - e^{-\frac{t}{\tau}}\right) \qquad (13)$$

$$o \leq t \leq t_1$$

$$t_1 >> \tau$$

$$T \doteq 2t_1$$

The maximum value of $R_{b1}(t)$ is then given by

$$R_{b1}(max) = R_o + QP_o \qquad (14)$$

Since $e^{-\frac{t}{\tau}}$ approaches its minimum value within a short time after $t = 0$, and since $t_1 >> \tau$, the detector output may be approximated by the result given in equation (14). The error introduced by these assumptions may be seen to increase rapidly as the ratio t_1/τ is reduced. The approximate shape of the output time response from the barretter under these conditions may be expected to be similar to that shown in Fig. 5b. If the barretter is operated with a constant current source, the video voltage appearing across the barretter with its resistance given by equation (14) will have a magnitude proportional to the incident microwave power level and a frequency equal to that of the modulating source. Note that the linearity of the time constant, τ, is not a factor in equation (14), but the power sensitivity constant, Q, is dependent upon the linearity of the coefficient of heat loss to the surroundings, γ, and the barretter coefficient of resistivity,

α. When typical barretter time constants are considered, it is obvious that the assumption $t_1 \gg \tau$ is a rather large restraint on the resulting frequency response of the detector. With typical time constants of 80 to 250 microseconds the video frequency response is severely limited. The condition $t_1 \gg \tau$ is not usually valid above about 2000 cycles per second. The result is that the barretter is of almost no value as an envelope detector except at these rather low frequencies. Hence, the response of the barretter to the common square pulse will not be very satisfactory for most applications.

With the condition that $T \geq 2t_1$ the interval between the two pulses will consist of a very rapidly decaying exponential as in Fig. 5b and will have no effect upon the next cycle. Under the given condition equation (12) may be approximated by

$$R_{b2}(t) = R_o + QP_o e^{-\frac{t - t_1}{\tau}} \qquad \text{for } t_1 \leq t \leq T \tag{15}$$

Since $t_1 \gg \tau$, this result very rapidly approaches the limit R_o, which is the bias resistance of the barretter. Again, the relatively large thermal time constants normally associated with these detectors allow the limiting solution, $R_{b2}(t) = R_o$, to be of practical value only at low modulating frequencies. Otherwise, the relation given in equation (15) is more appropriate.

With the condition that $t_1 \gg \tau$, the barretter as a video detector is often described as a "short time constant" detector.

The second special case is the approximation valid under the condition $t_1 \ll \tau \ll T$, that is the thermal time constant of the barretter element is much longer than the pulse width of the applied signal, but the interval between the pulses is sufficiently long to allow the barretter resistance to return to its original value prior to the next pulse. Under these conditions equation (11) for the resistance during the pulse may be approximated by

$$R_{b1}(t) = R_o + QP_o(1 - e^{\frac{-t}{\tau}}) \qquad o \ll t \ll t_1 \qquad (16)$$

A Taylor series expansion of equation (16) yields

$$R_{b1}(t) = R_o + \frac{QP_o t}{\tau}\left(1 - \frac{t}{\tau} - - - -\right)$$

The approximation $t_1 \ll \tau$ reduces this equation to

$$R_{b1}(t) = R_o + \frac{QP_o t}{\tau} \qquad (17)$$

Equation (17) evaluated at $t = t_1$ gives the total change in resistance, ΔR_b, equal to $\frac{QP_o t_1}{\tau}$. Thus, equation (17) may be normalized as

$$R_{b1}(t) = R_o + \frac{\Delta R_b}{t_1} t \qquad o \ll t \ll t_1 \qquad (18)$$

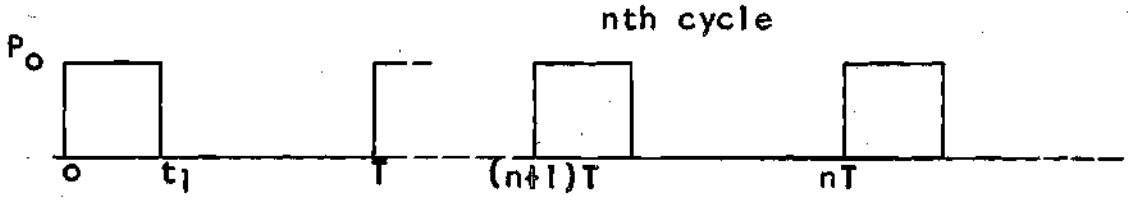

Figure 5a. Pulsed Microwave Signal Applied to the Barretter

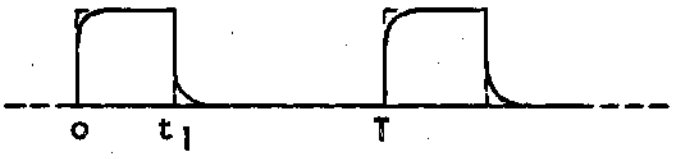

Figure 5b. Short Time Constant Detection, $\tau \ll t_1$

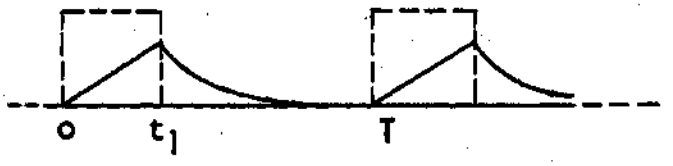

Figure 5c. Long Time Constant Detection, $\tau \gg t_1$

For the interval between pulses, the barretter resistance from equation (12) is approximated by

$$R_{b2}(t) = R_o + QP_o e^{-\frac{t-t_1}{\tau}} \left(1 - e^{-\frac{t_1}{\tau}}\right)$$

Again a Taylor series expansion gives

$$R_{b2}(t) = R_o + \frac{QP_o t_1}{\tau} \left(1 - \frac{t_1}{2\tau} - - - -\right) e^{-\frac{t-t_1}{\tau}}$$

which under the given conditions, $t_1 \ll \tau$, may be approximated by

$$R_{b2}(t) = R_o + R_b e^{-\frac{t-t_1}{\tau}} \tag{19}$$

The response of the barretter under the conditions given by equations (18) and (19) is shown in Fig. 5c. Equation (18) indicates that the change in barretter resistance is directly proportional to the product $P_o t$, the energy of the incident rectangular pulse. With a constant d-c bias current applied, a voltage is developed across the barretter terminals that is proportional to the energy stored in the detector. Therefore, the barretter with its time constant long in comparison with the applied pulse width is readily adaptable to applications of peak power measurements(13). Since $\tau = \frac{C_p}{\alpha}$, the barretter temperature variations under these conditions are dependent upon the specific heat and the thermal conductivity, which are in turn dependent upon the mass of the element. Thus, if the heat and the thermal conductivity of the barretter element are constant during the given pulse interval, the

temperature of the barretter may be expected to rise linearly with the energy supplied at a constant rate by the applied rectangular pulse. The barretter under these conditions is often described as a "long time constant" detector.

Differentiation of the voltage developed across the barretter under the conditions of the long time constant results in a signal that is proportional to the rate at which the thermal energy is stored in the detector, that is the instantaneous power applied to the detector. This differentiation results in the original envelope of the applied modulated signal. Then because of the good square-law characteristics of the barretter, this detected signal is proportional to the instantaneous power of the applied microwave signal. It has been shown (13) that a satisfactory peak power meter may be obtained by the use of the long time constant barretter followed by a differentiating circuit; the resulting signal is directly proportional to the power envelope of the applied pulse and a definite correlation exists between the amplitude of the output voltage and the incident microwave pulse. Fig. 6 shows the results to be expected from such a system.

The sensitivity of the barretter is reduced when used as the long time constant detector. Since only the initial slope of the resistance rise of the barretter is used, only a fraction of the total resistance variation is utilized, giving the rather large reduction in sensitivity. A reduction in the sensitivity of 50 per cent or greater is to be expected.

As a means of characterizing the long time constant detector, it has been proposed (13) that the pulse characteristics of the barretter may be best described in terms of the resistance rise created by a pulse of one milliwatt amplitude and of one microsecond duration. This resistance rise in ohms per milliwatt per microsecond is defined as the pulse sensitivity constant. The pulse sensitivity constant is the initial slope of the barretter response per milliwatt per microsecond and is defined graphically in Fig. 7.

Although the above discussion was limited to only the single problem of pulsed incident power, the general results obviously may be extended to other waveforms. It was shown that for the initial rise of the barretter response the detector output is proportional to the incident power and that by differentiation the original waveshape can be restored. This is true regardless of the waveshape, provided that the signal is pulsed and there is sufficient time between the pulses for the barretter resistance to return to its original biased conditions. Thus, during this limited time interval the incident pulse may have any form and still maintain a linear correspondence with the differentiated output. For many applications this is not too stringent a requirement.

Minimum Detectable Signal.--As with the crystal, the minimum detectable signal is defined as the input power level equal to the noise level of the system. If equation (26) in Appendix 2 is solved for the condition of the constant applied microwave

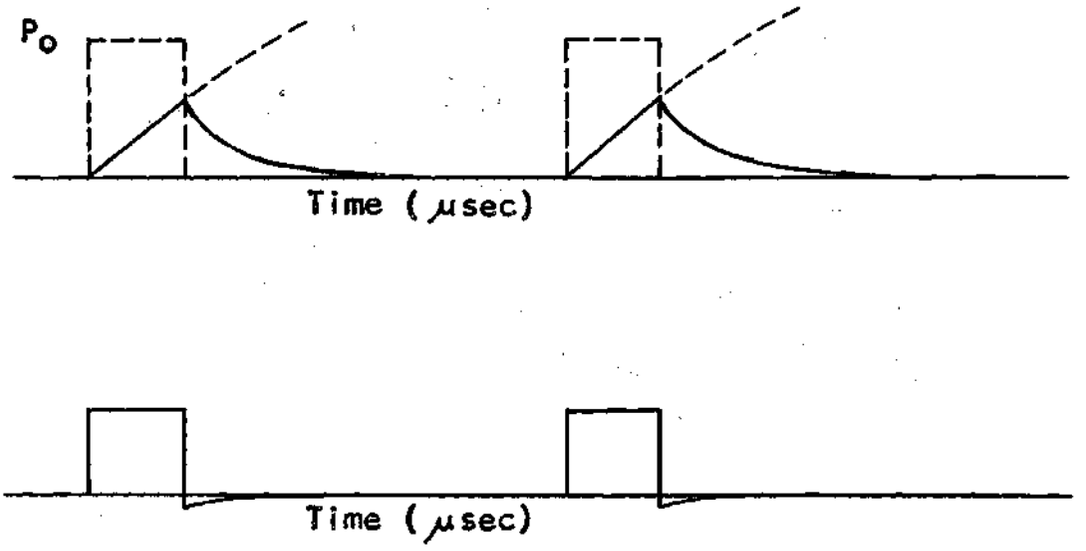

Figure 6. Detection by the Long Time Constant Barretter

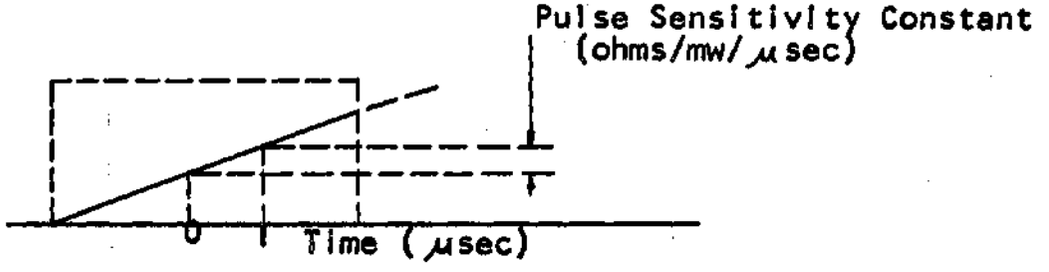

Figure 7. Pulse Sensitivity Constant Definition

power for time greater than some reference, (that is $P(t) = P_M$ for $t > t_o = 0$), the steady state solution for $R_b(t)$ after substituting into equation (39) is given by

$$R_b = R_o + QP_M$$

where $Q = \frac{\alpha}{\delta} R_o$ is defined with equation (40) in Appendix 2 to be the power-sensitivity constant. If the barretter is operating with a constant-current bias source, the output video signal is given by

$$v = i_b(R_o + QP_M)$$

The noise voltage for a system with a particular bandwidth and temperature is given in Appendix I to be

$$e = \sqrt{4KTR_oB_w}$$

Then the signal-to-noise ratio may be expressed as

$$\frac{S}{N} = \frac{i_bQP_M}{\sqrt{4KTR_oB_w}} \qquad (20)$$

since i_bR_o is the bias voltage applied to the barretter and i_bQP_o is the change in voltage output as a result of the applied microwave signal. Then if the signal-to-noise ratio is set equal to unity, the minimum detectable signal is given by

$$(P_M)_{min} = \frac{\sqrt{4KTR_oB_w}}{i_bQ} \qquad (21)$$

It is desirable to compare this result with that derived for the crystal in equation (8), where

$$(P_M)_{min} = \frac{\sqrt{4kTB_w}}{M}$$

The factor $\frac{i_b Q}{\sqrt{R_o}}$ is comparable with the figure of merit, M, used with the crystal and has the same units of volts per watt of incident power. Therefore, the minimum detectable signal is dependent upon the bias current, the barretter power-sensitivity constant, the system bandwidth, and the spectrum of the incident signal. This result is comparable with that for the crystal except that the crystal has no factor to compare with the bias current required with the barretter.

The bandwidth, B_w, is considered as a variable only in the sense of narrow bandwidth systems. Because of the rather long thermal time constant of the barretter the video response is very poor, limited to frequencies below approximately 2000 cycles, and the barretter is of little value as a wide band detector. Therefore, the barretter is normally operated as a narrow band detector.

By assuming for pulse modulation of the incident signal that the response of the barretter is perfect, (that is the square-law and the frequency response is ideal), it is possible to obtain a relationship between the maximum amplitude of the pulsed incident signal and the detected fundamental frequency that is passed through a narrow bandwidth detection system. By a Fourier expansion of the pulsed signal, the

voltage developed across the barretter as an even function is given by

$$v(t) = i_b Q P_o \left[\frac{q}{p} + \frac{2}{\pi} \sin\left(\frac{q}{p}\right) \cos\frac{\pi t}{p} \quad - - - - -\right]$$

where 2p is the period of the input signal and 2q is the pulse width. Then for a uniform square wave of p = 1 and q = $\frac{1}{2}$

$$v(t) = i_b Q P_o \left[\frac{1}{2} + \frac{2}{\pi} \cos\frac{\pi t}{p} \quad - - - - -\right] \tag{22}$$

Then if the system bandwidth is sufficiently narrow to pass only the fundamental, the rms voltage at the barretter output is given by

$$v_{rms} = \frac{\sqrt{2}}{\pi} \quad i_b Q P_o \tag{23}$$

This alters the result in equation (21) when only the fundamental component of the detected pulsed signal is available at the output and

$$P_{min} = \frac{\pi\sqrt{2KTR_b B_w}}{i_b Q} \tag{24}$$

The minimum detectable signal for Wollaston wire barretters are normally in the order of 10^{-4} microwatts.

Summary.--The characteristics that describe the barretter performance as a video detector or as a relative power indicating device may be summarized as follows:

1. For small changes in the applied power level a very good square-law response may be obtained over a wide dynamic

range.

2. Calibration may be easily accomplished and the resulting errors closely approximated.

3. The barretter has a theoretical minimum detectable signal in the order of 5×10^{-4} microvolts for a 25 cycle bandwidth.

4. The detector element itself is insensitive to frequencies below the maximum design frequency; the mount and associated circuitry introduce the frequency limitations.

5. Because of the relatively long thermal time constant, video detection is not practical above about 2000 cps.

6. With modulation pulses that are short as compared with the thermal time constant it is possible to obtain a direct relationship between the detected and applied signals within the barretter square-law limits. By differentiating the detected signal, good pulse reproduction with a square-law response may be obtained but with a loss in sensitivity.

CHAPTER IV

TEST PROCEDURES AND APPLICATIONS

Laboratory Equipment.--Several methods have been established for the measurement of many of the characteristics of the crystal and barretter detectors(11). The laboratory tests outlined below were conducted to verify several of the important characteristics of the detectors outlined in Chapters II and III; the objective was not to establish new or unique techniques of measurements. These tests should substantiate the general theory of the operation of these detectors and together with the remainder of this report provide a sufficiently complete analysis that these detectors may be more completely understood with respect to each other in their respective applications. However, the results obtained here are intended to be only typical and should not be applied directly to a particular application without proper consideration.

The crystals and barretters used in the laboratory tests were taken from available commercial types. A summary of the characteristics to be expected from these detectors are given in Table 1; this gives an indication of the results that may be expected.

The basic laboratory test system is shown in Fig. 8. The VSWR meters that were used as the output device in many of the tests have very narrow amplifier bandwidths that are

Table 1. Detector Characteristics*

	Crystals	Bolometers
Minimum Signal (For a 25 cycle bandwidth	9×10^{-6} microwatts	5×10^{-4} microwatts
Range of Square-Law (Noise to 2% deviation from square-law	Noise to 0.25 microwatts	Noise to 200 microwatts
Db Variation from Noise to 2% deviation from square-law	44 db	56 db
Usable db Variation (10 times noise to 2% deviation from square-law for the 25 cycle bandwidth)	34 db	46 db
Microvolts/microwatt	5000	21
Bias Source	None	Requires d-c bias
Video Time Constant	Approximately 0.002 microseconds exclusive of r-f bypass and external wiring	80 to 250 microseconds

*Courtesy Polytechnic Research and Development Company(8)

tuned to 1000 cps. Therefore, the modulator for the test oscillator must have its fundamental frequency tuned to the mid-frequency of the video amplifier band pass. The modulation signal used was a square wave with very fast rise and decay time; this was necessary to allow a rapid transition of the oscillator to the condition of full operation and to reduce the chance of modulation distortion. In determining the incident power at the detector mount it was necessary to make several assumptions; this results in an unknown error but one that should be acceptable for these tests. First, it was necessary to assume that the power absorbed by the barretter element used with a power bridge is the microwave power incident upon the mount. Then it was assumed that the microwave power detected by the barretter is the same as that detected by the crystal when the two detectors are interchanged in the same mount with optimum tuning. These errors are in addition to the normal errors experienced in power measurements(11). The power bridge was used to establish a particular reference power level at the detector mount by varying the uncalibrated attenuator in Fig. 8. Then the power bridge was removed and the output indicating device used in its place. The calibrated attenuator was then used to provide the required variation in the input power. All measurements were made in db or dbm.

The first crystal detector shown in Fig. 8 was used as a power monitor, that is the power level of the input to the

variable attenuators was observed for any variations in the oscillator output or for any effect from overloading. The nonlinear characteristics of this crystal were not of importance since the applied power level stayed essentially constant and only an indication of a variation in power level was required. A wave meter was also inserted here to measure the frequency of the microwave oscillator.

Three separate test systems were used, as may be seen in Fig. 8, with 10,000, 35,000, and 70,000 megacycles per second as the approximate frequencies of operation. The test set-up for the three systems was basically the same. An interchangeable detector mount was used at 10,000 mcps but separate mounts were required for the crystal and barretter for the other two systems. An E-H tuner was placed between the detector mount and the wave guide in all tests to provide an additional variable in controlling the microwave impedance match.

Essentially the same tests were performed on both types of detectors and at each frequency. The tests were intended to demonstrate more clearly the correlation between the crystal and the barretter as video detectors and toshow the similarity at the three frequencies.

The Crystal.--The dynamic response for the 1N23B crystel at 10,600 mc. with a 200 ohm load is given in Fig. 9. The general shape of the output voltage curve may be seen to be similar to curve C in Fig. 1. Hence, this crystal with a

200 ohm resistive load has a square-law response to approximately -25 dbm; then the response curve rises above 2 to a maximum close to 3 and decreases to its large signal limit of 1. In the region between the limiting cases of small and large signals there is not a smooth transition from the square-law to the linear detection. As stated in Chapter II, the variation in the detection law, or the exponent given in equation (6), is dependent upon the crystal parameters and the load resistance. The results of similar tests on two othercrystal types is shown in Fig. 10 for a load resistance of 200 ohms. Although the curves are not identical, the general shape is the same; that is, the square-law response of the detector extends to a maximum power level of about -25 to -30 dbm. There is a sufficient difference in the crystals that it is not possible to obtain a general calibration curve and expect any reasonable accuracy from crystal to crystal, even within the same type. At the power levels larger than approximately the maximum of the response curve given in Fig. 10, the power series approximation given in equation (2) is no longer adequate. At these higher power levels the crystal spreading resistance (the resistance caused by the transition from the small point contact to the larger semiconductor body) is no longer negligible and considerably influences the crystal response(5).

Although the response curve in Fig. 9 is obtained as an experimental plot of the output video voltage as a function of the power incident upon the detector, the response could just

as well have been given by a plot of the detector circuit output current as a function of the relative magnitude of the transmission line voltage or field strength. This latter approach is not preferred since it is difficult to define voltage in waveguides at these frequencies.

No qualitative information may be obtained from these tests about the maximum frequency limits of these particular crystals. The operation of the crystal at these frequencies appear normal and in agreement with that to be expected. At the higher frequencies it is more difficult to obtain dependable results because of the additional losses and attenuation that are present and the more critical tuning required.

As discussed in Chapter II, the impedance mismatch between the crystal and the transmission line is related to the incident power level. Hence, it is necessary to retune the mount at each power level of incident power. The effect of not tuning the crystal mount and the E-H tuner is shown in an approximate result in Fig. 11. This curve indicates that the error introduced by this impedance mismatch is more pronounced at the higher power levels where the deviation of the crystal response from the square-law is greater. The error introduced by this mismatch over the dynamic range given in Fig. 11 was found to be in the order of 0.8 to 1.0 db. However, if the crystal is operated within the limits of its square-law range (to a maximum of about -30 dbm), the effect of this error is usually negligible.

As indicated by equation (7) it should be possible to obtain a unique value of the load resistance that will extend the square-law response beyond the limits indicated in Fig. 10 by as much as 10 to 15 db. In addition, this equation gives a theoretical means of determining the actual voltage applied across the crystal. Fig. 13 shows how the response law for the 1N21 crystal varies as a function of a varying load resistance. The result for this crystal is in agreement with similar tests performed on the 1N21B and 1N26 (6,7). For the 1N21B it was found that optimum response was obtained with a resistive load of 11,400 ohms; the optimum response for the 1N26 corresponded to approximately 3900 ohms. The load resistance obtained for the 1N21B by experiment agreed favorably with that obtained by equation (7) discussed above(7). The results obtained in Fig. 13 were obtained by placing a 5000 ohm potentiometer in series with the input to the VSWR meter as shown in Fig. 12.

Although the square-law response may be improved by the proper choice of the load resistance, this is not so simply done. There is no assurance that the desired response curve is obtained with good accuracy unless a check is made on each crystal because of the variations in the crystal parameters. In addition, there is an increase in the system noise with the increasing load resistance that limits the minimum power level of operation. This effect may be seen in Fig. 13.

With both the microwave and video impedance match influencing the crystal detection law, it seems impossible to obtain optimum response with varying input power and frequency with a fixed-tuned crystal mount.

The video response of the crystal is also dependent upon the value of the video load as stated in Chapter II. The relation between the video response and the square-law response is such that it is generally not possible to obtain optimum conditions for both with one value of the load resistance. With the aid of the small positive bias shown in Fig. 12 it is possible to improve considerably the video response of the crystal. Fig. 14 gives the video response of a 1N53 crystal at 35,000 mc. with a varying bias. This shows a considerable improvement of the pulse response with very little reduction in sensitivity.

The Barretter.--For small changes in its operating temperature, the barretter is a very good approximation to a square-law detector. The experimental static responee of two barretter detectors is shown in Fig. 15; this shows that the square-law response is very closely approximated by the barretter for relatively small changes in applied power over a wide dynamic range. The sensitivity of these detectors may be obtained from the static curve; both these curves have a typical sensitivity of about 13 ohms per milliwatt of applied power. Thus, the power sensitivity constant, Q, in equation (12) has a value of 13 ohms per milliwatt for these barretters. The approximate

output voltage sensitivity may be obtained by the product of the bias current and the above resistive sensitivity. Thus, for a bias current of 4.7 milliampers there is a total voltage variation of 61 millivolts output per applied milliwatt of power.

The deviation from the desired square-law response in Fig. 15 may be determined approximately by extending a tangent from the given operating point and measuring the per cent deviation from square law $= \frac{\Delta R_T - \Delta R}{\Delta R_T} (100)$, where ΔR_T is the ideal square-law resistance variation per increment of applied power, and ΔR is the actual variation of the barretter resistance for this increment of applied power. Variations in the order of one per cent per milliwatt are to be expected.

Below the design frequency limits, the d-c heating effects approximate very closely the microwave heating; therefore, the dynamic response of the barretter will be very close to that obtained by the static test. Fig. 16 gives a plot of the experimental results obtained which should be typical of the results to be expected for all barretters. Note that on a loglog graph there appears to be a linear relation between the error and the actual barretter response. Thus, if the barretter bias is properly adjusted and if the detector is not overloaded, the resulting error may be approximated from these two curves. This is the error resulting from the deviation from the square-law response; this must be added to the other

system errors(10).

In Chapter III the two limiting cases are discussed that describe the barretter as a useful instrument; that is the conditions for the long and short time constant applications. Most often only the short time constant (the barretter time constant short relative to a period of the applied signal) application is considered as practical. Fig. 17 gives the response of three barretters operating as "short time constant" detectors. From these curves it was calculated that the thermal time constants were approximately 60 microseconds, 60 microseconds, and 80 microseconds respectively for the PRD617 at 35,000 mcps, for the PRD634 at 70,000 mcps, and for the N821B at 10,000 mcps. Hence one sees that barretter time constants are in the range of 60 to 80 microseconds; this restricts the frequency components of the applied signal to below a maximum of about 2000 cps if an acceptable response is to be obtained. This is a rather severe restriction. The barretter is therefore useful as an envelope detector only for the less common low frequency applications. The barretter may, however, be used as a power detector for various waveshapes providing the period of the fundamental component of the incident signal is long compared to the detector time constant. Then as indicated in Chapter III, it is possible to establish a relation between the detected fundamental component and the incident signal provided its approximate waveshape is known.

The other limiting case of the long time-constant detector requires that the barretter time constant be long as compared with the period of the reoccurring incident signal. Fig. 18 shows the response obtained experimentally for a particular barretter operated under these conditions. The response shown is in very close agreement with the results predicted by equations (18) and (19). During the interval of the pulse, the response of the barretter was very nearly a linear output as predicted. The sensitivity for this output signal cannot be determined as easily as the static or steady-state sensitivity which applies for the short time constant response. However, as stated in Chapter III if this output is linear for the duration of the pulse, the response and the sensitivity can be determined from the initial slope of the barretter response by use of equation (11). Therefore, the pulse sensitivity constant as defined in Fig. 7 may be theoretically obtained by differentiating the output given in equation (11), and evaluating the output at $t = 0$ to obtain the initial slope. This states that the pulse sensitivity constant is dependent upon the barretter time constant, τ, and the power sensitivity constant, Q, for long time-constant conditions. The initial slope under these conditions is given by

$$\frac{d}{dt} R_{bl}(0) = \frac{Q}{\tau} P_o$$

For the barretter used as an example above, the values of $Q = 13$ ohms per milliwatt and $\tau = 80$ microseconds predict a pulse sensitivity of 0.163 ohms per milliwatt per microsecond. With a bias current of 4.7 millampers the pulse voltage sensitivity was then 0.761 millivolts per milliwatt per microsecond. This compares very closely with the results obtained by laboratory experiment. The steady-state sensitivity was measured to be 60 millivolts per milliwatt for the PRD 617 barretter in Fig. 17 and its time constant was measured to be approximately 80 microseconds; therefore, the voltage pulse-sensitivity was 0.75 millivolts per milliwatt per microsecond. Thus, the results obtained by static measurements are sufficiently close to the dynamic results that the characteristics may be determined by static measurements and the barretter theory given in Chapter III. The maximum output voltage to be expected from the barretter operating as a long-time-constant detector is given by the product of the above pulse voltage-sensitivity and the pulse width of the applied signal.

Applications.--Several of the common applications of the crystal and the barretter discussed at points throughout the above text may now be summarized with respect to their general characteristics.

The VSWR measurement is one that often utilizes both the crystal and the barretter. In general, the barretter is more suitable for this task since only a relative measurement

is required and the same waveform is present throughout the test. The square-law characteristic of the barretter allows a relatively accurate measurement for small values of the VSWR. Several techniques have been advanced for obtaining very acceptable results(11). However, at very low power levels the barretter sensitivity is not adequate and the crystal is preferred. The crystal is acceptable at power levels below about -30 dbm since it has an approximate square-law response in this range and has a much greater sensitivity (250:1) than the barretter. Thus, if care is taken to insure the power variations applied across the crystal do not surpass this upper limit, the crystal will give acceptable results at these lower power levels; the barretter may be used as a complementary device for power levels above the acceptable range of the crystal because of its greater dynamic range. If possible, the barretter is always to be preferred for any type of relative power measurement because it is a closer approximation to the true square-law detector over its entire range.

The requirements for attenuation measurements are about the same as with the VSWR. The barretter is preferred except at the low power levels where the barretter sensitivity will not yield a sufficient output and the crystal is an approximately square-law device. Large values of attenuation should be measured with care, using either detector, since the large variation in power levels may introduce considerable error if the detector operation expands into the power level region for which it is not a suitable detector.

In general, the crystal may be used for two types of applications: those that require square-law power detection and those that require a good video response. As compared with the barretter the crystal is able to provide a much better video response and is thus better adapted for modulation detection. Although the response is influenced considerably by the crystal load, the response may be improved by applying a small d-c bias or by the proper choice of the load resistance. The crystal video response is normally significantly better than may be obtained by other detection methods. However, the crystal operating as a modulation detector does not allow a direct correspondence between the magnitudes of the incident and applied signals.

CHAPTER V

SUMMARY

As indicated in Chapter I, it is perhaps not too profitable to compare directly the crystal and the barretter without first studying the basic differences in the two methods of detection. Once the basic characteristics are known, the utility of each detector for any particular application may then be very easily determined.

First, it was pointed out that the crystal is a point-contact type of rectifier while the barretter is an electrical to thermal energy converter yielding a change in resistance that is the consequence of a change in temperature. Neither device is a transducer in that it does not generate the electrical output; the crystal performs as an electronic rectifier and the barretter merely modulates a flow of current. The major difference in the two detectors is primarily dependent upon their respective means of detection. In comparison with the thermal time constant of the barretter, the crystal has a much shorter time constant (a no load time constant of about 10^{-3} microseconds as compared with that of about 80 microseconds for the barretter) which gives the crystal a relatively good video response. The second major factor is the dynamic response law; the crystal is able to maintain its square-law response only at the very low power levels (noise to about

-30 dbm) while the barretter has an approximate square-law response for small changes in temperature over its entire realizable power spectrum. These characteristics may not be completely stated this simply. The video and power response of the crystal is acutely dependent upon the video load; the optimum video response occurring for an infinite impedance and the optimum square-law response occurring for a unique video resistance in the order of a few thousand ohms. Thus, it is not possible to obtain both the maximum square-law and video response simultaneously. However, an additional improvement in the video response with a slight decrease in sensitivity may be obtained with the addition of a small d-c bias. The video response of the barretter is a function of the thermal time constant; this may be reduced to a sizable degree only by decreasing the physical heat capacity of the barretter element (metallic films as used in radiation measurements is an example).

An important characteristic of the crystal is its very good sensitivity with respect to other video detectors. At the frequencies in the order of 10,000 mcps the crystal sensitivity is about 250 times greater than the sensitivity of the barretter. However, because of the increasing influence of the barrier resistance and shunt capacity at the shorter wavelength, the sensitivity of the crystal decreases considerably with decreasing wavelength and approaches that of the barretter at the millimeter wavelengths. Because of this greater

sensitivity the crystal has a minimum detectable signal that may be as much as 15 to 20 db below that of the barretter. At the low power levels where the crystal is a square-law detector, the crystal is preferred over the barretter as a square-law detector because of its greater sensitivity.

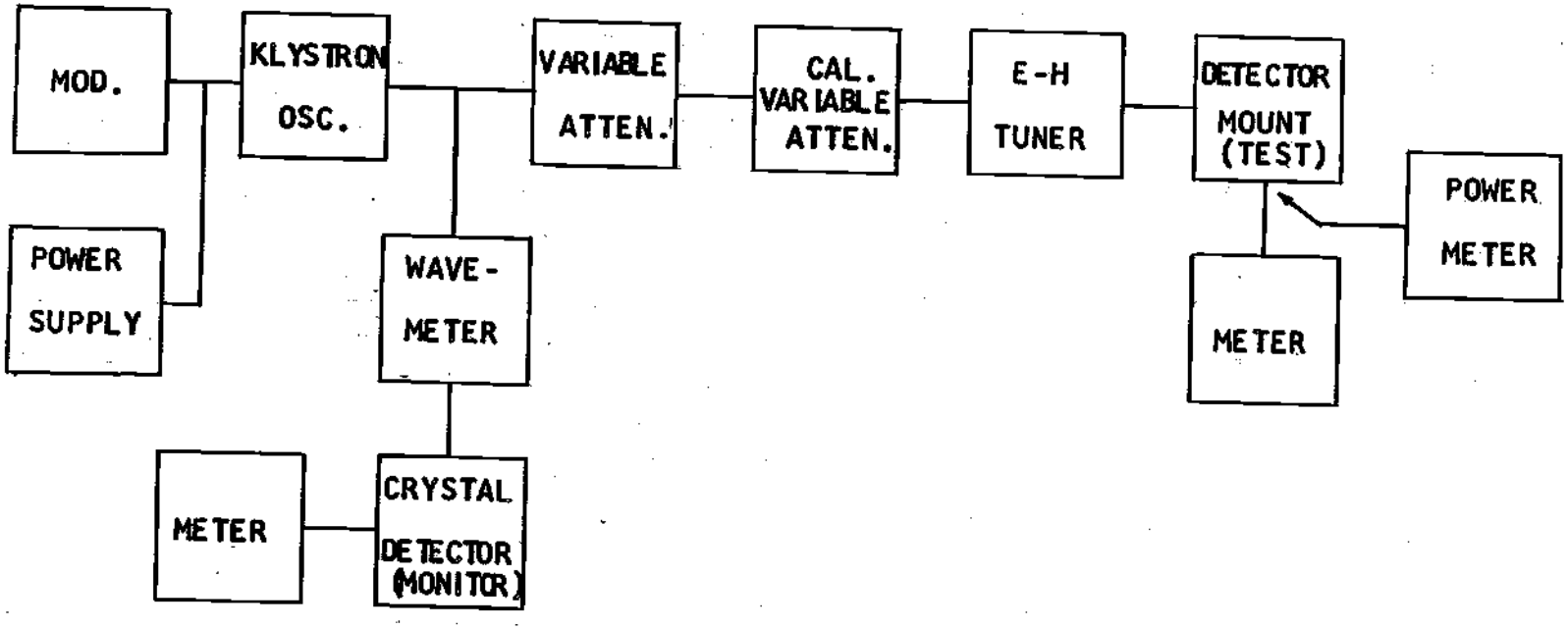

Figure 8. Laboratory Test System

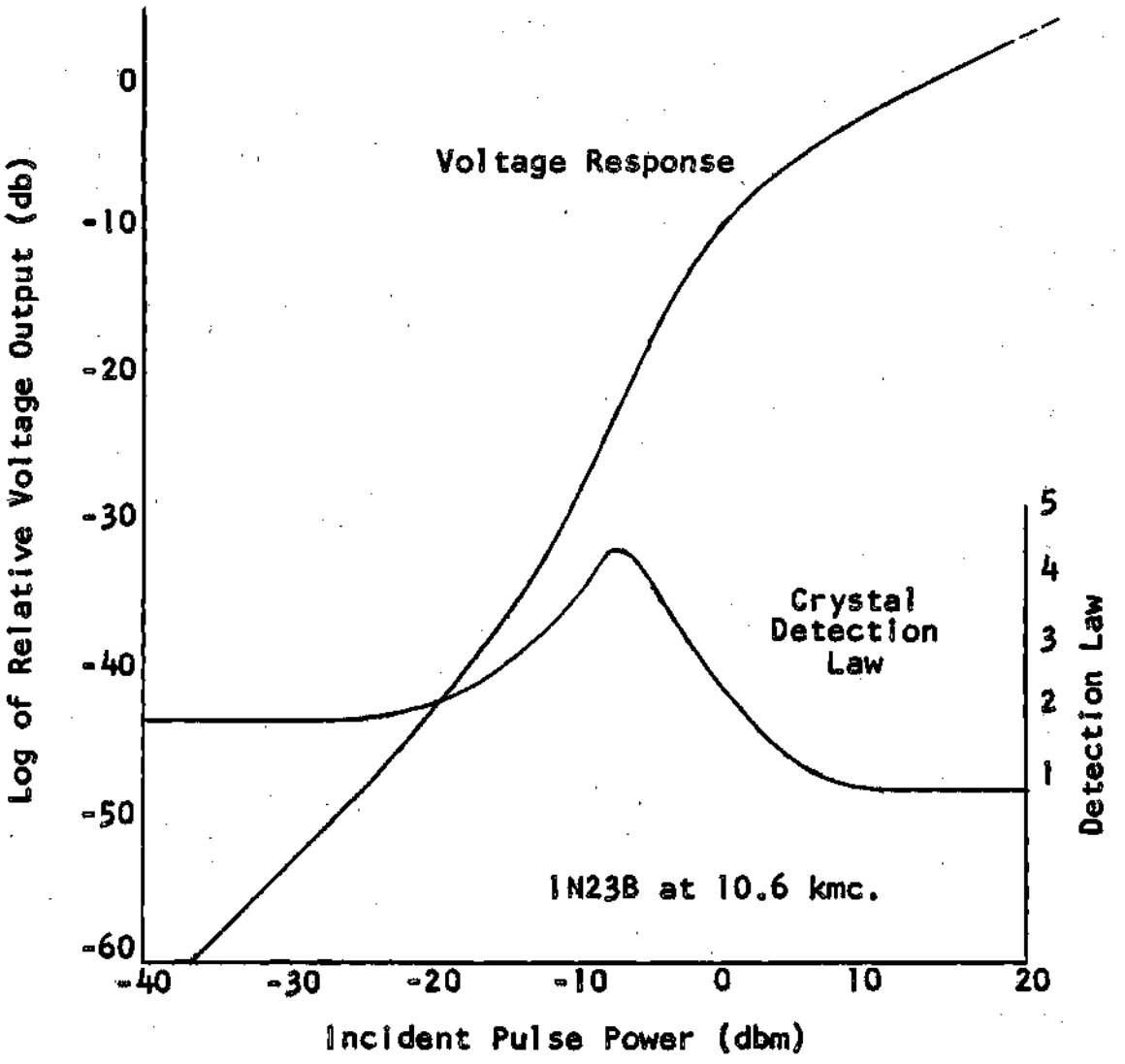

Figure 9. Crystal Output Voltage and Dectection Law as a Function of the Applied Power

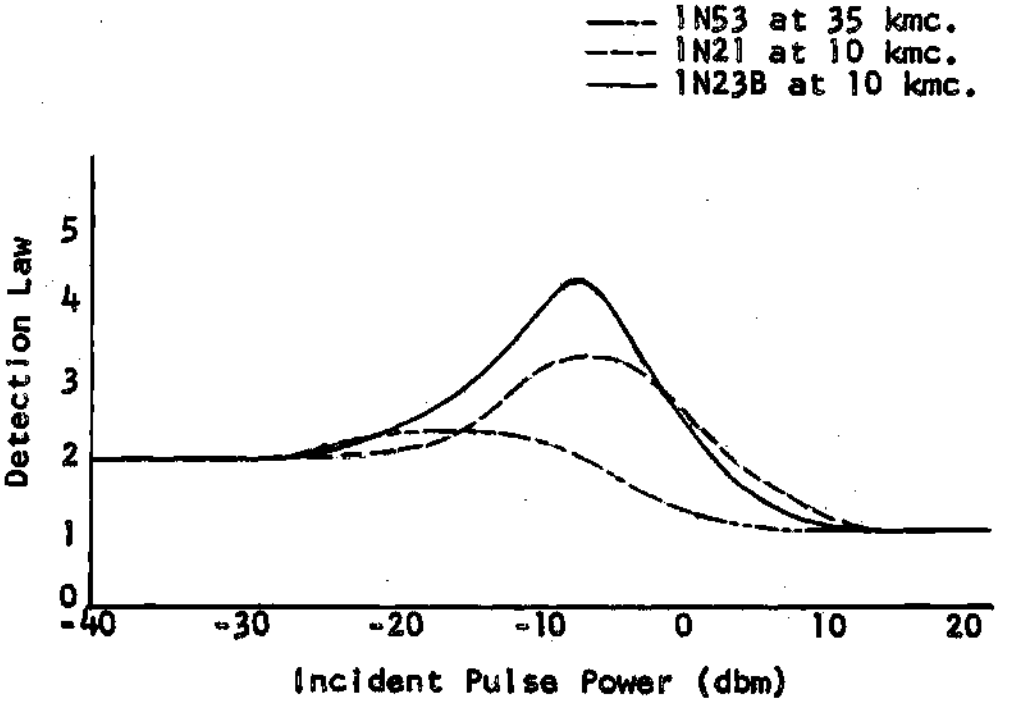

Figure 10. Comparison of three Crystal Detection Laws

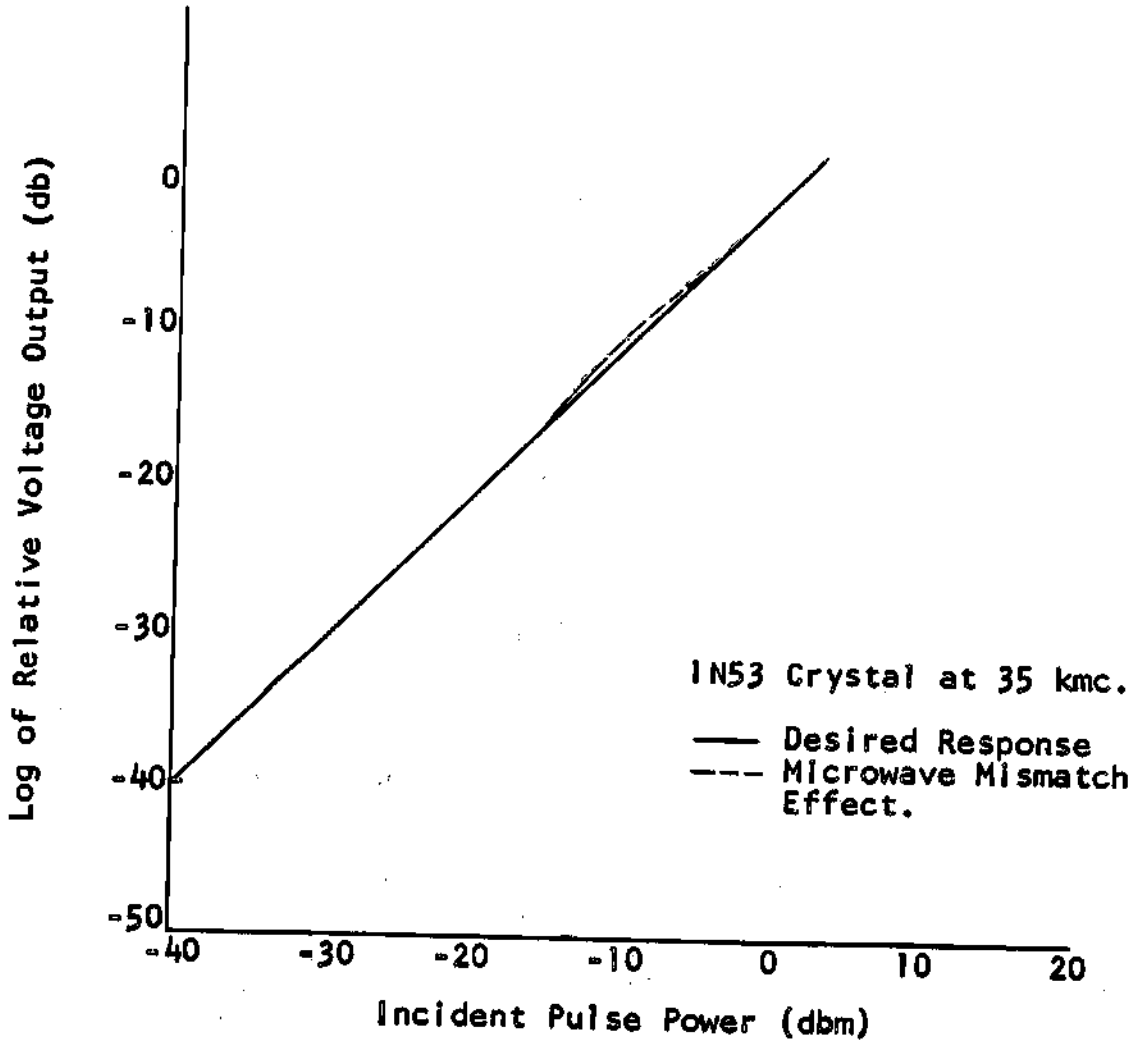

Figure 11. Effect of Microwave Impedance Mismatch

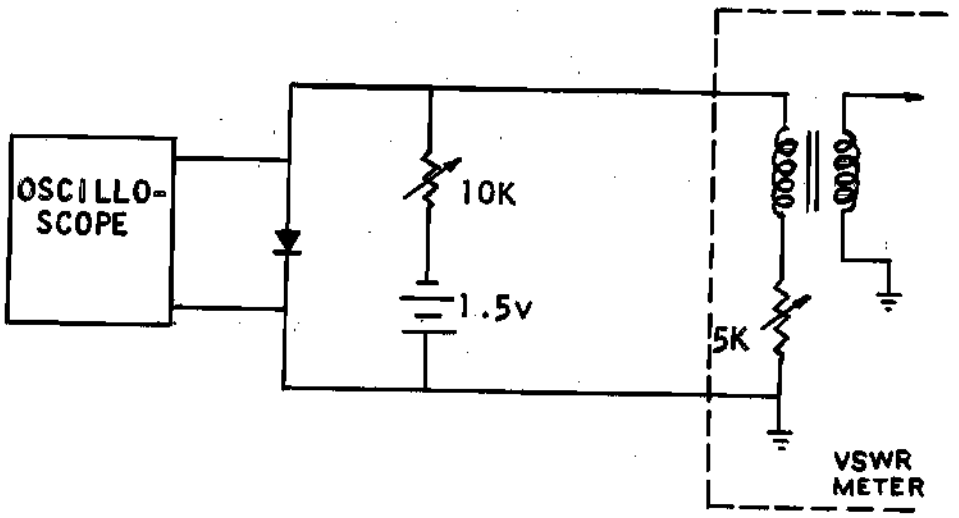

Figure 12. Test System for the Crystal Bias and Video Load

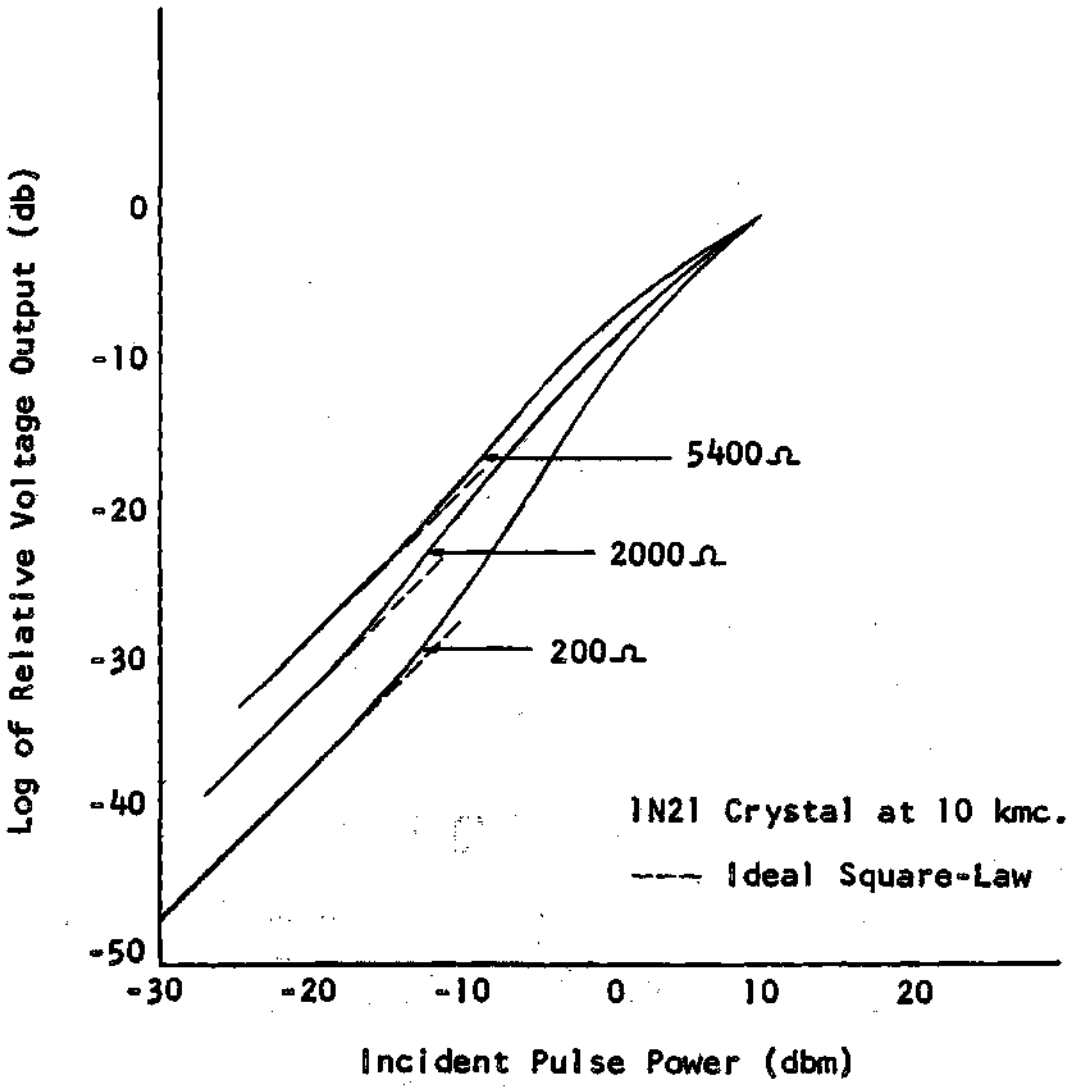

Figure 13. Crystal Response as a Function of its Video Load

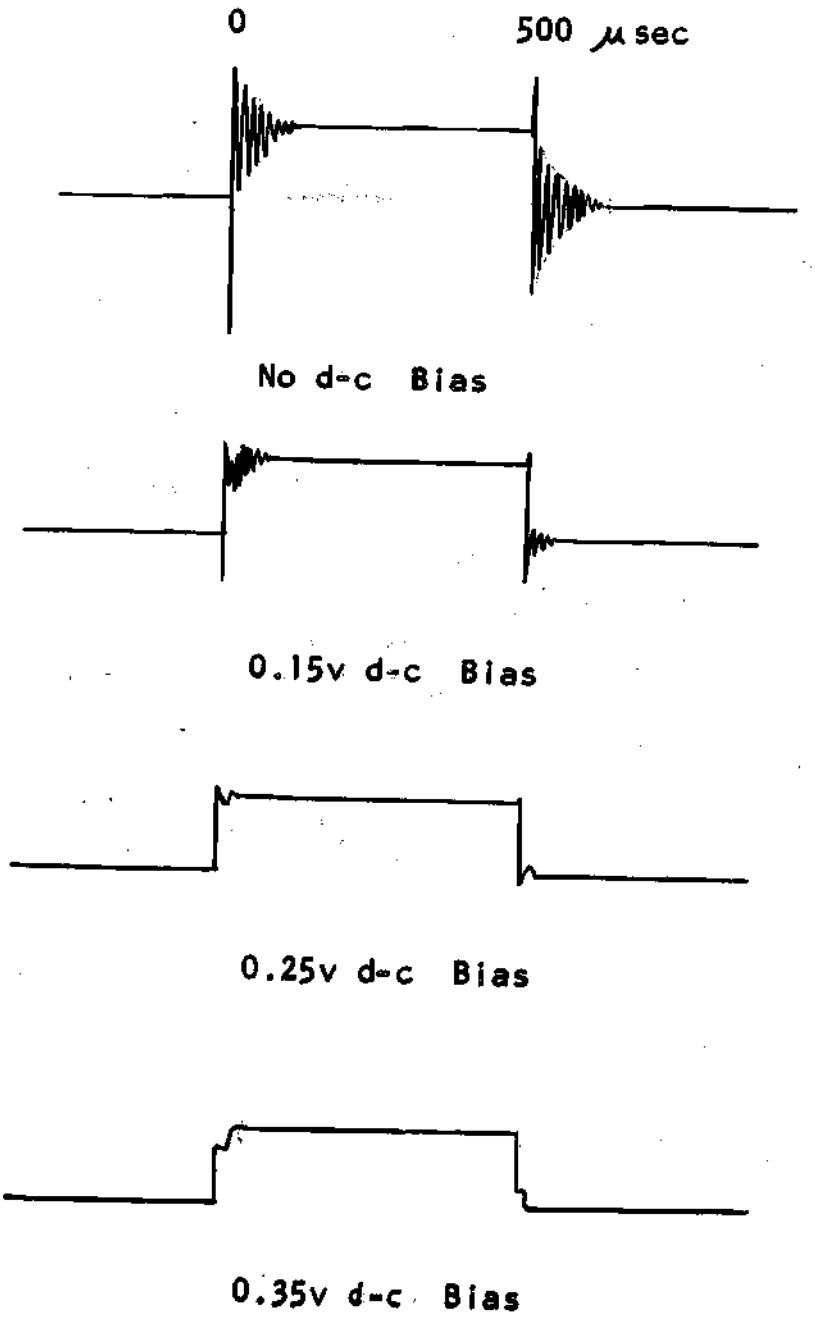

Figure 14. Effect of D-C Bias Voltage on Crystal Performance

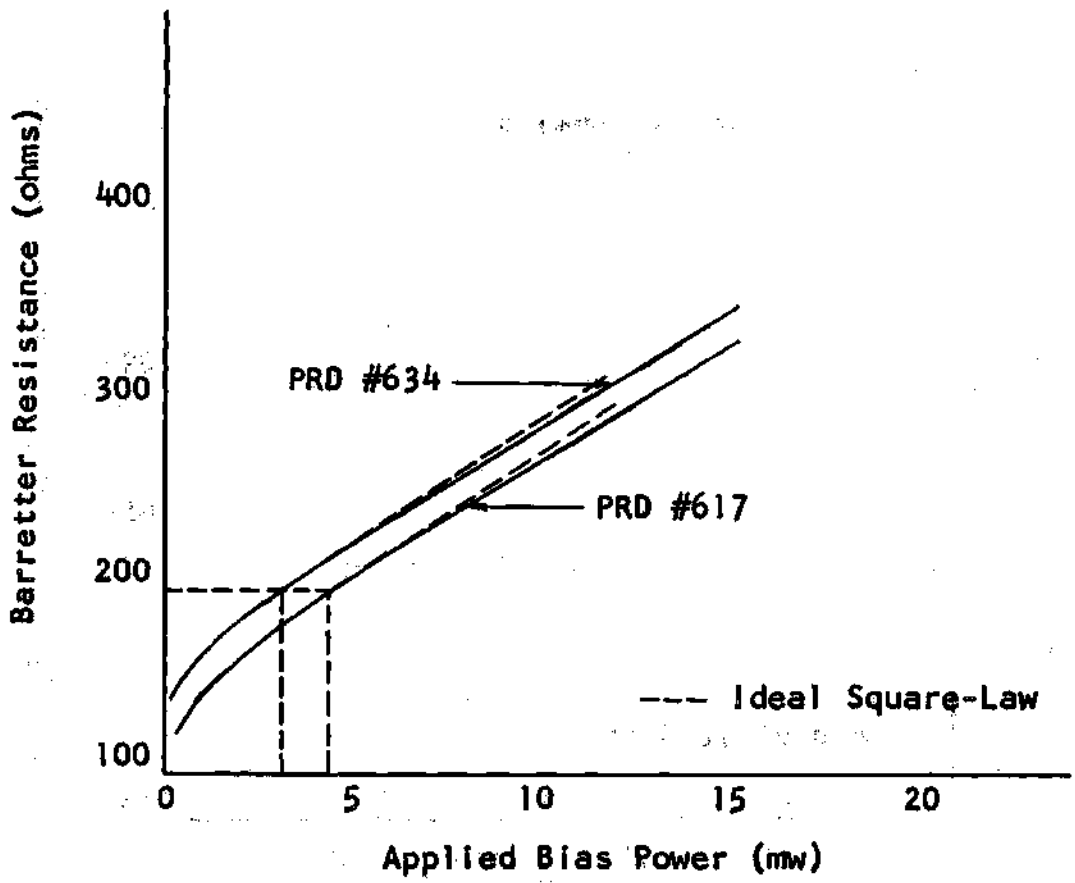

Figure 15. Barretter Static Characteristic Curves

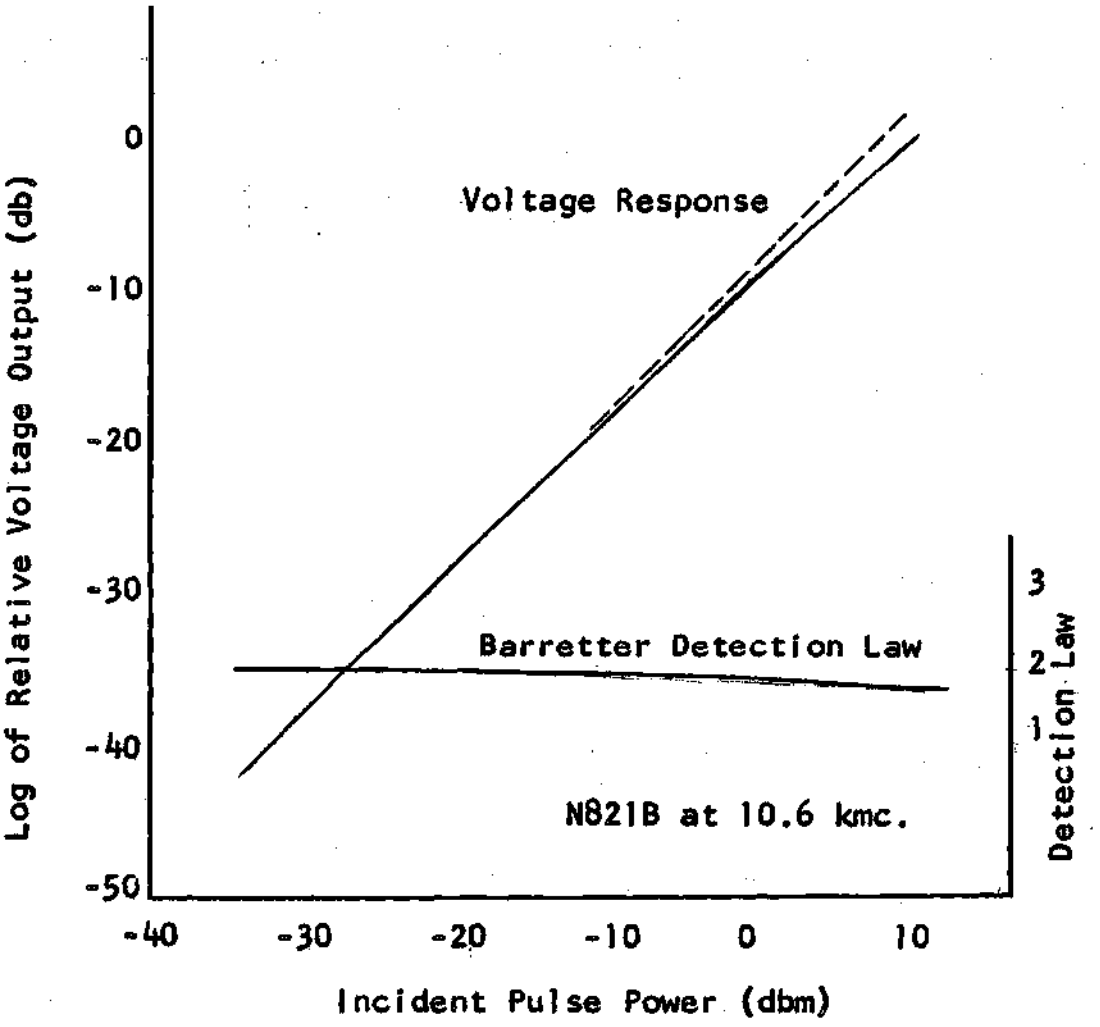

Figure 16. Barretter Output Voltage and Detection Law as a Function of the Applied Power

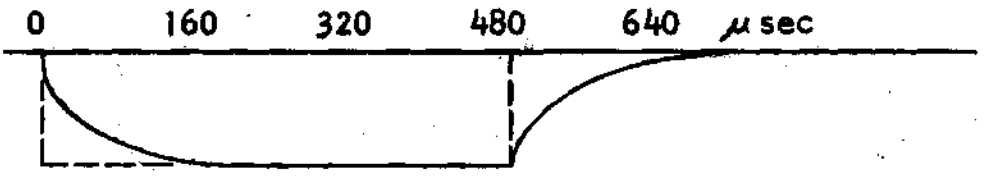

PRD 617 Response at 35 kmc.

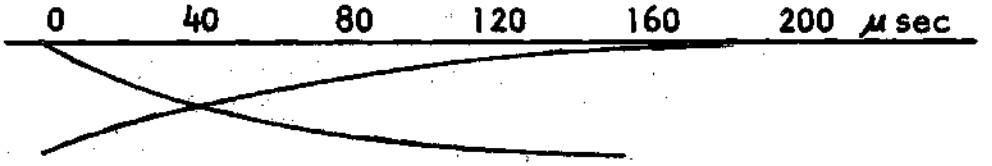

Comparison of the Above Rise and Decay Transients

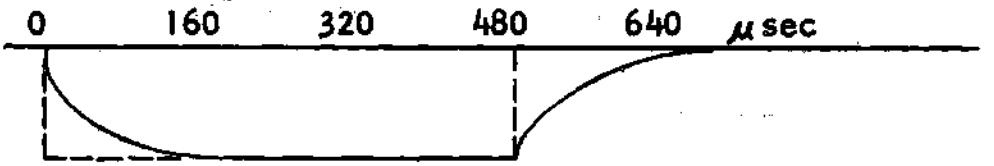

PRD 634 Response at 70 kmc.

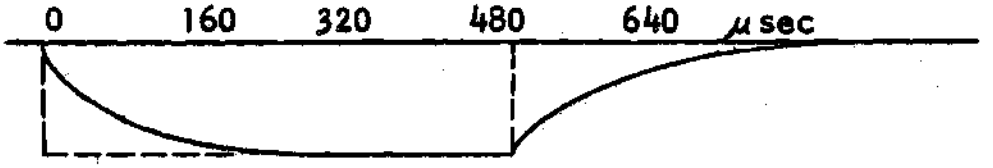

N821B Response at 10 kmc.

Figure 17. Comparison of Three Barretter Pulse Responses

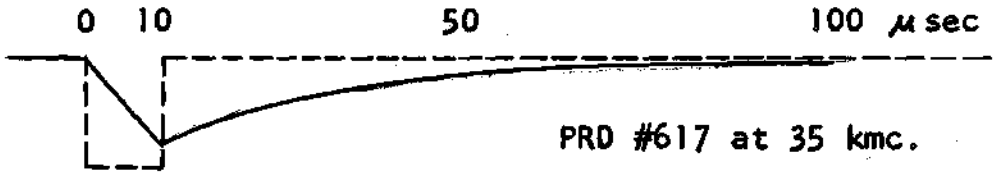

Direct Barretter Response

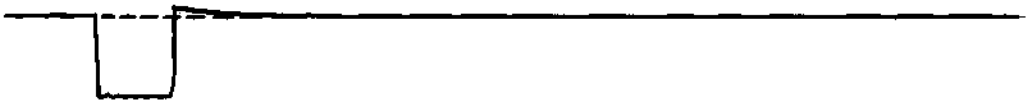

Differentiated Barretter Response

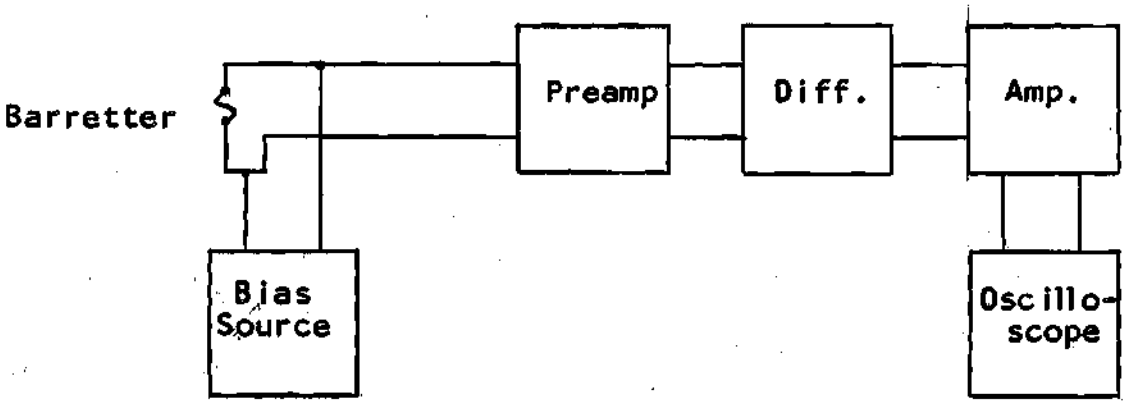

Figure 18. Short Pulse Detection with the Long Time Constant Barretter

APPENDICES

APPENDIX 1

FIGURE OF MERIT

The figure of merit, M, is related to the video resistance of the crystal and to its current sensitivity. This parameter is defined in an attempt to obtain a general characteristic of the crystal performance as a video detector. The figure of merit is proportional to the signal-to-noise ratio of the crystal and is determined by the rectification properties and the noise generation of the crystal.

To determine the figure of merit, measurements are required of the crystal video resistance and short circuit current (or current sensitivity) and the equivalent noise resistance of the video amplifier used with the crystal must be known. In general, the figure of merit only yields information on the detector performance at the single incident power level and thus does not furnish all the information needed to describe the crystal.

A crystal detector under the desired ideal square-law conditions will pass a current proportional to the microwave power, P_M, given by

$$i = SP_M$$

where S = current sensitivity of the crystal (microamperes

per microwatt). The no load output voltage will then be given by

$$V_{oc} = R_V S P_M$$

where R_V is the shunt video resistance of the equivalent crystal current source.

With no signal input (or bias) the crystal is in thermo-dynamic equilibrium and the video noise for the low level operation is almost entirely the Johnson noise of a resistance equal to the shunt video resistance of the crystal (plus some effect from the input resistance, R_a, to the first stage). Hence, the squared noise voltage output, e_n^2, is given by

$$e_n^2 = 4KT\,(R_V + R_a)\,B_W$$

where K = Boltmann's constant = 1.38 x 10-3 joules/sec

T = absolute temperature in ^{o}K

B_W = bandwidth in cycles

Then the open circuit signal-to-noise ratio (S/N) may be defined as

$$\frac{S}{N} = \frac{R_V S P_M}{\sqrt{4KT(R_V + R_a)B_W}}$$

$$= \frac{MP_M}{\sqrt{4KTB_W}} \qquad (25)$$

where $M = \frac{SR_v}{\sqrt{R_v - R_a}}$ is defined as the crystal figure of merit. This S/N ratio could also apply to the output of the amplifier since the major noise generating element, R_a, and the bandwidth of the amplifier have been included in the above expressions. Also note that with constant input power the M is proportional to the system signal-to-noise ratio.

APPENDIX 2

DERIVATION OF THE BARRETTER RESPONSE

Assume that the pulsed microwave power incident upon the barretter element is of the form shown in Fig. 5, where P_o is the maximum value of the applied power pulse and t_1 is the width of each pulse.

An approximation to the heat equation for the barretter element under the conditions given for microwave video detection may be given by (10)

$$c_p \frac{d}{dt} u(t) + \gamma u(t) = P(t) \qquad (26)$$

where $u(t)$ is the temperature rise in the barretter, c_p is the barretter heat capacity, γ is the coefficient of heat loss to the surrounding and $P(t)$ is the time dependent power incident upon the barretter. Define $u_1(t)$ as the barretter temperature during the power pulse as given in Fig. 5a and $u_2(t)$ as the barretter temperature between the pulses. Also for the nth cycle of the applied pulse train assume that $t = 0$ corresponds to $t = (u-1)T$, that is the origin is shifted to the beginning of the nth cycle. Then during the pulse of the nth cycle, equation (26) may be written as

$$P_o = c_p \frac{d}{dt} u_1(t) + \gamma u_1(t)$$

Applying the Laplace Transform to the equation given above, the result is given as

$$U_1(S) = \frac{P_o}{\gamma}\left(\frac{1}{S} - \frac{1}{S + \frac{\gamma}{c_p}}\right) + \frac{u_1(n)}{S + \frac{\gamma}{c_p}}$$

Therefore

$$U_1(t) = \frac{P_o}{\gamma}\left(1 - e^{-\frac{\gamma}{c_p}t}\right) + u_1(n)\, e^{-\frac{\gamma}{c_p}t}$$

This result applies to the nth cycle and the time constant may be defined as $\tau = \frac{c_p}{\gamma}$

For the time interval between pulses, assume another time shift so that $t = (n - 1)T + t_1$ corresponds to $t = 0$. Equation (26) may be rewritten under these conditions as

$$P(t) = o = c_p \frac{d}{dt} u_2(t) + \gamma u_2(t)$$

$$o = c_p S u_2(S) - c_p u_2(t_1) + \gamma u_2(S) \qquad (28)$$

However, since the temperature of the barretter cannot change immediately, $u_2(t_1) = u_1(t)$. Substituting the $t = t_1$ into equation (27) results in the following equation which is then substituted into equation (28).

$$u_1(t) = \frac{P_o}{\gamma}\left(1 - e^{-\frac{t}{\tau}}\right) + u_1(n)e^{-\frac{t_1}{\tau}}$$

$$u_2(t) = \frac{P_o}{\gamma}\left(1 - e^{-\frac{t_1}{\tau}}\right)e^{-\frac{t-t_1}{\tau}} + u_1(n)e^{-\frac{t}{\tau}} \qquad (29)$$

It is necessary to shift equation (29) back to the origin given with equation (27) by replacing t with $t - t_1$, giving

$$u_2(t) = \frac{P_o}{\gamma} \left(1 - e^{-\frac{t_1}{\tau}}\right) e^{-\frac{t-t_1}{\tau}} + u_1(n)e^{-\frac{t}{\tau}} \qquad (30)$$

Note in Fig. 4 that at $t = T$, $u_2(t) = u_2(T) = u_1(n + 1)$. Therefore, rewriting equation (30)

$$u_1(n + 1) - u_1(n)e^{-\frac{T}{\tau}} = \frac{P_o}{\gamma} \left(1 - e^{-\frac{t_1}{\tau}}\right) e^{-\frac{T-t_1}{\tau}} \qquad (31)$$

This is the first order difference equation of the form (14)

$$u_1(n + 1) - au_1(n) = b \qquad (32)$$

This may be rewritten in the ordinate form as

$$\left[u_1(u + 1) - a \right] u_1(n) = \left[b \right]$$

Applying the Laplace Transform, this reduces to

$$e^w \left[u_1(w) - u_1(n = o)\ P\ (w)\right] - au_1(w) = \frac{b}{w}$$

where $u_1(n = 0)$ corresponds to the initial temperature of the barretter. However, since u(t) is defined as the temperature rise of the barretter, $u_1(n = 0)$ must equal zero. Therefore

$$u_1(w) = \frac{b}{w(e^w - a)}$$

$$u_1(t) = \frac{b}{a - 1} \left[(a^n - 1)\right.$$

for n equal to integral values only, the "jump" may be removed,

$$u_1(n) = \frac{b(a^n-1)}{a-1}$$

With the constant $u_1(n)$ now evaluated, the relations for the barretter temperature may be obtained for both during and between the applied pulses. Hence, equations (27) and (30) may be written as

$$u_1(t) = \frac{P_o}{\delta}\left(1 - e^{-\frac{t}{\tau}}\right) + \frac{b(a^n - 1)}{a - 1} e^{-\frac{t}{\tau}} \qquad (33)$$

$$u_2(t) = \frac{P_o}{\delta}\left(1 - e^{-\frac{t_1}{\tau}}\right) e^{-\frac{t-t_1}{\tau}} + \frac{b(a^n-1)}{a - 1} e^{-\frac{t}{\tau}} \qquad (34)$$

Equations (33) and (34) above give the temperature of the barretter element at any given time during or between pulses of the nth cycle of the applied microwave signal as given in Fig. 5. Since for all practical purposes the applied signal may be assumed to be recurring, the steady-state solution for the nth cycles is adequate. Therefore, it is necessary to remove the transient component from the above equation. First, referring to equations (31) and (32) it is possible to obtain

$$b(a^n-1) = \frac{P_o\left(e^{\frac{t_1}{\tau}} - 1\right)\left(1 - e^{\frac{nT}{\tau}}\right) e^{-\frac{nT}{\tau}}}{\delta\left(1 - e^{\frac{T}{\tau}}\right)} \qquad (35)$$

Substituting this into equations (33) and (34) yields

$$u_1(t) = \frac{P_o}{\gamma}\left[1 - e^{-\frac{t}{\tau}}\left(1 - \frac{(e^{\frac{t_1}{\tau}} - 1)(e^{-\frac{nT}{\tau}} 1\ 1)}{1 - e^{\frac{T}{\tau}}}\right)\right] \tag{35}$$

$$u_2(t) = \frac{P_o}{\gamma}\ e^{-\frac{t}{\tau}}\left[e^{\frac{t_1}{\tau}} - 1 + \frac{(e^{\frac{t_1}{\tau}} - 1)(e^{-\frac{nT}{\tau}} - 1)}{1 - e^{\frac{T}{\tau}}}\right] \tag{36}$$

The transient portion of this solution may be removed by assuming that $n \gg 1$, that is the pulse train is very long as compared with one cycle. It is then obvious that $nT \gg T$, and since $T > t_1$, it must be also true that $nT \gg t_1$. Making this simplification, equation (35) and (36) will reduce to the following steady-state solutions:

$$u_1(t) = \frac{P_o}{\gamma}\left(1 - e^{-\frac{t}{\tau}}\ \frac{1 - e^{-\frac{T-t_1}{\tau}}}{1 - e^{-\frac{T}{\tau}}}\right) \quad \text{for } o \leq t \leq t_1 \tag{37}$$

$$u_2(t) = \frac{P_o}{\gamma}\left(\frac{1 - e^{-\frac{t_1}{\tau}}}{1 - e^{-\frac{T}{\tau}}}\ \ e^{-\frac{t-t_1}{\tau}}\right) \quad \text{for } t_1 \leq t \leq T \tag{38}$$

where $t=0$ corresponds to the beginning of a cycle.

The resistance of the barretter as a function of time may be related to its temperature by

$$R_b(t) = R_o\ \left[1 + \alpha\, u(t)\right] \tag{39}$$

where α is the temperature coefficient of resistivity of the barretter. The steady-state variations of the barretter may

therefore be given approximately by the following pair of equations:

$$R_{b1}(t) = R_o + QP_o \left(1 - e^{-\frac{t}{\tau}} \frac{1 - e^{-\frac{T-t_1}{\tau}}}{1 - e^{-\frac{T}{\tau}}} \right) \qquad (40)$$

$$R_{b2}(t) = R_o + QP_o \left(\frac{1 - e^{-\frac{t_1}{\tau}}}{1 - e^{-\frac{T}{\tau}}} \right) e^{-\frac{t-t_1}{\tau}} \qquad (41)$$

where $Q = \frac{R_o \alpha}{\gamma}$ is defined as the barretter power sensitivity constant.

BIBLIOGRAPHY

BIBLIOGRAPHY

1. Terman, F. E., Radio Engineer's Handbook, McGraw-Hill Book Company, Inc., 1943.

2. Van Voorhis, S. N., Microwave Receivers, Massachusetts Institute of Technology Radiation Laboratory Series, Vol. 23, McGraw-Hill Book Company, Inc., 1948.

3. Rubin, S. W., "Millimeter Waves," Polytechnic Research and Development Company, Inc., Report, Vol. 4, No. 3, October, 1955.

4. Sharpless, W. M., "Wafer-Type Millimeter Wave Detectors," Bell System Technical Journal, Vol. 35, 1956.

5. Torrey, H. C., and C. A. Whitmer, Crystal Rectifiers, Massachusetts Institute of Technology Radiation Laboratory Series, Vol. 15, McGraw-Hill Book Company, Inc., 1948.

6. Henning, R. E., Microwave Peak Power Measurement Technique, Unpublished Ph. D., Thesis, Columbia University, 1954.

7. Flesher, G. T., "The Crystal Constant in Microwave Measurements," Proceedings of the National Electronics Conference, Vol. IX, National Electronics Conference, Inc., 1953, p. 911.

8. Laskin, H. J., "Microwave Detectors for Measurements of Relative Power Levels," Polytechnic Research and Development Company, Inc., Report, Vol. 3, No. 1, July, 1954.

9. Cheng, D. K., "A Note on the Reproduction of Pulse," Proceedings of Institute of Radio Engineers, Vol. 40, August, 1952, pp. 962-66.

10. Sucher, M., and H. J. Carlin, "The Operation of Bolometers Under Pulsed Power Conditions," Transactions of Institute of Radio Engineers, Vol. PGMTT-3, No. 4, July, 1955, pp. 45-52.

11. Montgomery, C. G., Technique of Microwave Measurements, Massachusetts Institute of Technology Radiation Laboratory Series, Vol. 11, McGraw-Hill Book Company, Inc., 1948.

12. Soloman, C., "Microwave Power Measurements," Polytechnic Research and Development Company, Inc., Report, Vol. 1, No. 4, January, 1953.

13. Henning, R. E., "Microwave Peak Power Measurements," Private communication.

14. Gardner, M. F., and J. L. Barnes, Transients in Linear Systems, Vol. I, John Wiley and Sons, 1942.

Other References

Barlow, H. M., and A. L. Cullen, Microwave Measurements, Constable and Company, 1950.

Beatty, R. W., and A. C. Macpherson, "Mismatch Errors in Microwave Power Measurements," Proceedings of Institute of Radio Engineers, Vol. 41, September, 1953, pp. 1112-19.

Billings, B. H., W. L. Hyde, and E. E. Barr, "An Investigation of the Properties of Evaporated Metal Bolometers," Journal of the Optical Society of America, Vol. 37, March, 1947, p. 123.

Billings, B. H., W. L. Hyde, and E. E. Barr, "Construction and Characteristics of Evaporated Nickel Bolometers," Review of Scientific Instruments, Vol. 18, June, 1947, p. 429.

Hund, A., High Frequency Measurements, McGraw-Hill Book Company, Inc., 1951.

Jones, R. C., "The General Theory of Bolometer Performance," Journal of the Optical Society of America, Vol. 43, pp. 1 - 14, 1953.

Jones, R. C., "Performance of Detector for Visible and Infrared Radiation," Advances in Electronics, Vol. V., Academic Press, 1953.

Macpherson, A. C., and D. M. Kerus, "A New Technique for the Measurement of Microwave Standing-Wave Ratios," Proceedings of Institute of Radio Engineers, Vol. 44, August, 1956, pp. 1024-32.

Mendel, J. T., "Microwave Detector," Proceedings of Institute of Radio Engineers, Vol. 44, Part 1, April, 1956, pp. 503-09.

Moreno, T., and O. C. Landstrom, "Microwave Power Measurements," Proceedings of Institute of Radio Engineers, Vol. 35, May, 1947, pp. 514-18.

Sorrows, H. E., W. E. Ryan, and R. C. Ellenwood, "Evaluation of Coaxial Slotted-Line Impedance Measurements," Proceedings of Institute of Radio Engineers, Vol. 39, February, 1951, pp. 162-68.

Strum, P. D., "Some Aspects of Mixer Crystal Performance," Proceedings of Institute of Radio Engineers, Vol. 41, July, 1953, pp. 875-90.